UC Irvine
Faculty Publications

Title
The southern ocean at the Last Glacial Maximum: A strong sink for atmospheric carbon dioxide

Permalink
https://escholarship.org/uc/item/2wc5k4d0

Journal
Global Biogeochemical Cycles, 14(1)

ISSN
08866236

Authors
Moore, J. Keith
Abbott, Mark R
Richman, James G
et al.

Publication Date
2000-03-01

DOI
10.1029/1999GB900051

Copyright Information

Peer reviewed

The Southern Ocean at the last glacial maximum: A strong sink for atmospheric carbon dioxide

J. Keith Moore,[1] Mark R. Abbott, James G. Richman, and David M. Nelson

Oregon State University, College of Oceanic and Atmospheric Sciences

Abstract. Analysis of satellite ocean color, sea surface temperature, and sea ice cover data reveals consistent patterns between biological production, iron availability, and physical forcings in the Southern Ocean. The consistency of these patterns, in conjunction with information on physical conditions during the last glacial maximum (LGM), enables estimates of export production at the LGM. The LGM Southern Ocean experienced increased wind speeds, colder sea surface and atmospheric temperatures, increased deposition of atmospheric dust, and a greatly expanded winter sea ice cover. These variations had strong effects on Southern Ocean ecology and on air-sea fluxes of CO_2. The seasonal ice zone (SIZ) was much larger at the LGM (30 million km^2) than at present (19 million km^2). The Antarctic Polar Front (PF) likely marked the northern boundary of this expanded SIZ throughout the Southern Ocean, as it does today in the Drake Passage region. A large northward shift in the position of the PF during glacial times is unlikely due to topographic constraints. North of the PF, the increased flux of aeolian dust during glacial times altered phytoplankton species composition and increased export production, and as a result this region was a stronger sink for atmospheric CO_2 than in the modern ocean. South of the PF, interactions between the biota and sea ice strongly influence air-sea gas exchange over seasonal timescales. The combined influence of melting sea ice and increased aeolian dust flux (with its associated iron) increased both primary and export production by phytoplankton over daily-monthly timescales during austral spring/summer, resulting in a strong flux of CO_2 into the ocean. Heavy ice cover would have minimized air-sea gas exchange over much of the rest of the year. Thus, an increased net flux of CO_2 into the ocean is likely during glacial times, even in areas where annual primary production declined. We estimate that export production in the Southern Ocean as a whole was increased by 2.9 - 3.6 Gt C yr^{-1} at the LGM, relative to the modern era. Altered seasonal sea ice dynamics would further increase the net flux of CO_2 into the ocean. Thus the Southern Ocean was a strong sink for atmospheric CO_2 and contributed substantially to the lowering of atmospheric CO_2 levels during the last ice age.

1. Introduction

Martin [1990] argued that the Southern Ocean surrounding Antarctica was a much stronger sink for atmospheric carbon dioxide (CO_2) at the last glacial maximum (LGM) due to an increase in phytoplankton primary production driven by elevated fluxes of iron from continental dust sources to surface waters. This process was termed the iron hypothesis for explaining the observed lowering of atmospheric CO_2 during the last ice age [*Martin,*

1990]. Several analyses of the sedimentary record have argued for lower Southern Ocean primary production at the LGM and concluded that the Southern Ocean was not a strong sink for CO_2 at that time [*Mortlock et al.,* 1991; *Charles et al.,* 1991; *Shemesh et al.,* 1993; *Nürnberg et al.,* 1997]. In this paper, we present new data and arguments, which suggest that the Southern Ocean was indeed a strong net sink for atmospheric CO_2 at the LGM, due to increased phytoplankton production during spring/summer months and reduced outgassing of CO_2 during winter months due to heavy sea ice cover. Our analysis is based largely on the current understanding of modern Southern Ocean ecosystems supplemented with satellite measurements of ocean color and sea ice distributions. Recent analyses of satellite sea surface temperature data allows new insights into the dynamics and location of the Antarctic Polar Front (PF) in the modern and glacial oceans [*Moore et al.,* 1997; 1999a]. The arguments presented here are consistent with the known sedimentary record from the Southern Ocean. Interactions between sea

---

[1]Now at National Center for Atmospheric Research, Boulder, Colorado.

ice and the biota over seasonal timescales are critical to reconciling the iron hypothesis with the sedimentary record.

The physical environment of the Southern Ocean at the LGM, ~21,000 years ago (earlier references cite 18,000 years ago based on ^{14}C dating, see Bard et al. [1990]), was very different from that in today's ocean. The ice age Southern Ocean was marked by cooler sea surface temperatures (SST), an expanded winter sea ice extent, colder surface air temperatures (~9°C degrees lower on the Antarctic continent), and an increase in the deposition of atmospheric dust (~15-20 fold) [Hays, 1978; Climate: Long-Range Investigation, Mapping, and Prediction (CLIMAP), 1981; Petit et al., 1981, 1990; Jouzel et al., 1987; Pichon et al., 1992]. In addition, atmospheric CO_2 levels were at ~200 ppm, ~80 ppm lower than the modern preindustrial average, and sea level was 120-150 m lower [Barnola et al., 1987; Crowley, 1988].

A role for the high latitude oceans (in particular the Southern Ocean) in the ice age lowering of atmospheric CO_2 has been proposed by numerous authors [e.g., Knox and McElroy, 1984; Siegenthaler and Wenk, 1984; Sarmiento and Toggweiler, 1984; Keir, 1988; Broecker and Peng, 1989; Martin, 1990]. Model results demonstrate that primary production levels in the Southern Ocean can strongly influence atmospheric CO_2 levels [i.e., Sarmiento and Orr, 1991; Joos and Siegenthaler, 1991; Sarmiento and Le Quéré, 1996]. Martin [1990, 1992] and Martin et al. [1990a, 1990b] suggested release from iron limitation by increased atmospheric deposition as a mechanism for increased Southern Ocean productivity at the LGM.

Atmospheric dust levels were much higher at the LGM [Petit et al., 1981, 1990]. This increased dust deposition was a global phenomenon with greatly increased dust inputs relative to modern times recorded in Greenland and Antarctica ice cores [Petit et al., 1981; De Angelis et al., 1997]. Petit et al. [1981] found continental aerosol flux on the Antarctic continent was ~ 20 times higher at the end of the last glacial period. Similarly, Petit et al. [1990] estimated that mean dust flux to the Antarctic continent at the LGM was 15 times higher than Holocene levels. Kumar et al. [1995] found that iron flux to the sediments in the South Atlantic increased by more than a factor of 5 at the LGM.

Several studies have examined chlorophyll distributions in the Southern Ocean using the previous generation ocean color sensor, the Coastal Zone Color Scanner (CZCS) [Comiso et al., 1993; Sullivan et al., 1993]. The CZCS studies, new data from the Sea-viewing Wide Field-of-view Sensor (SeaWiFS) and in situ measurements indicate that phytoplankton blooms where chlorophyll concentrations > 1.0 mg m^{-3} are restricted primarily to three regions. These "bloom regions" include coastal and shelf waters, areas near the receding edge of the seasonal ice sheet, and waters in the vicinity of the major hydrographic fronts [Lutjeharms et al., 1985; Tréguer and Jacques, 1992; Laubscher et al., 1993; Comiso et al., 1993; Sullivan et al., 1993; Banse, 1996; Moore et al., 1999b; this study].

Ecological structure is fundamentally different in the blooming and nonblooming regions of the Southern Ocean. In the bloom regions, phytoplankton biomass is dominated by larger diatom species, although Phaeocystis (a prymnesiophyte) can be an important component in Antarctic coastal, shelf, and ice edge waters. These species are able to escape grazing control by their predators, typically larger

zooplankton, i.e., krill and copepods, which have long generation times compared to the phytoplankton. These bloom regions tend to have high f ratios and export production [Tréguer and Jacques, 1992; Banse, 1996]. The f ratio, the ratio of new production to total production, represents the fraction of phytoplankton production available for export from the surface layer over annual timescales [Dugdale and Goering, 1967; Eppley and Peterson, 1979].

In contrast to these spatially restricted bloom regions, large portions of the Southern Ocean have perpetually low chlorophyll concentrations where smaller nano-sized and pico-sized phytoplankton dominate [Treguér and Jacques, 1992; Banse, 1996]. These areas have lower f ratios, low export production, and perpetually high macronutrient concentrations (phosphate 1.5 > μM and nitrate > 20 μM south of the PF) [Comiso et al., 1993]. The microzooplankton that graze upon these smaller phytoplankton size have generation times comparable to those of phytoplankton and, thus, maintain a tight grazing control on phytoplankton biomass [Sherr and Sherr, 1994]. A similar situation exists in the equatorial Pacific, another high-nutrient, low-chlorophyll (HNLC) region [Landry et al., 1997].

The bloom regions have elevated dissolved iron concentrations relative to other areas of the Southern Ocean, at least part of the time [Martin et al., 1990a, b; de Baar et al., 1995; Sedwick and DiTullio, 1997; Sedwick et al., 1997]. Bottle incubation experiments indicate that offshore phytoplankton respond to iron additions with increased growth rates and biomass and with a shift in species composition toward larger diatoms [Martin et al., 1990b; Hebling et al., 1991; de Baar et al., 1995; Van Leeuwe et al., 1997; Scharek et al., 1997; Takeda, 1998]. These results imply that increasing iron levels in situ would increase export production, as happens in the other HNLC areas [Coale et al., 1996; Gordon et al., 1997; Hutchins et al., 1998; see also Sunda and Huntsman, 1997].

Recently, the Southern Ocean Iron Release Experiment (SOIREE) provided further evidence that waters south of the PF are indeed iron limited [Boyd et al., 1999]. In this experiment a large patch of seawater (at 141°E, 61°S) was fertilized with iron additions over a 13-day period, and a suite of measurements was made both within the iron-fertilized patch and in adjacent waters. Over this period, chlorophyll levels increased markedly, and the pCO$_2$ of surface waters decreased in the iron-enriched patch [Boyd et al., 1999]. This experiment provides dramatic evidence that the availability of iron limits phytoplankton biomass accumulation within the Southern Ocean today.

Martin [1990] suggested that atmospheric dust that accumulates on sea ice, releases substantial amounts of iron to the water column as the ice melts, thus enhancing phytoplankton growth. Sedwick and DiTullio [1997] recently reported evidence of such iron fertilization by melting sea ice in the Ross Sea. The input of low-salinity meltwater also increases vertical stratification of the water column, improving the irradiance/mixing regime for phytoplankton [Smith and Nelson, 1986].

An important concept for the arguments presented here is the effect of iron limitation on uptake ratios of macronutrients by diatoms. Recent studies have demonstrated that uptake ratios of silica/nitrate and silica/phosphorus are 2-3 times higher under iron-limitation than under iron-replete conditions [Takeda, 1998; Hutchins

and Bruland, 1998; Hutchins et al., 1998]. Since the phytoplankton maintain Redfield ratios between carbon, nitrogen, and phosphorus [Redfield et al., 1963], silica/carbon ratios within cells are also 2-3 times higher under iron-limitation, a fact noted previously by Martin [1992]. These results suggest that percent opal and biogenic opal accumulation rates may not be reliable proxies of export production in the Southern Ocean over glacial-interglacial periods, as the amount of iron input to surface waters varied drastically [Takeda, 1998]. Such paleoproxies may underestimate glacial diatom production by more than 50% [Takeda, 1998]. Thus increases in export carbon of 100% or more could go unrecorded in the opal sediment record [Martin, 1992].

In this paper we discuss the likely ecological consequences of increased atmospheric dust flux and the greatly expanded seasonal sea ice extent at the LGM and the subsequent effects on air-sea CO_2 fluxes. Our analyses are based largely on satellite-derived estimates of sea ice cover, chlorophyll distributions, and frontal dynamics in the modern Southern Ocean. We use a broad definition for the Southern Ocean, encompassing the area from the North Subtropical Front to the Antarctic continent. Our methods for processing the satellite data and some assumptions are outlined in section 2. In section 3 we examine phytoplankton biomass and primary productivity patterns in the modern Southern Ocean incorporating new satellite ocean color data from SeaWiFS. In section 4, we review air-sea CO_2 fluxes in the modern Southern Ocean. Seasonal sea ice dynamics are critical to our arguments. We examine sea ice distributions in the modern ocean and at the LGM and their relationship to the Antarctic Polar Front in sections 5 and 6.

We examine the ecology of the Southern Ocean at the LGM in section 7. We propose that the expansion of the seasonal ice sheet and the increased aeolian iron flux at the LGM resulted in an ecological regime shift within the whole area south of the PF toward a pattern similar to that observed in the southern Weddell and Ross Seas of the modern ocean. This would lead to increased export production during austral spring and summer, and reduced outgassing of CO_2 during winter. In section 8 we discuss the implications of this ice age Southern Ocean ecology for net air-sea CO_2 fluxes and, finally, the role of the Southern Ocean in the observed glacial atmospheric CO_2 decrease.

2. Methods and Materials

SeaWiFS-derived estimates of surface chlorophyll concentration for the period October 1997 through September 1998 were obtained from the Goddard Space Flight Center [McClain et al., 1998]. Daily level 3 standard mapped images of chlorophyll concentration (Version 2) were averaged to produce monthly and seasonal means for the Southern Ocean.

Monthly mean sea ice concentrations (NASA Team algorithm) from the Nimbus-7 Scanning Multichannel Mircrowave Radiometer (SMMR) and DMSP-F8, -F11, -F13 satellite sensors for the years 1978-1998 were obtained from the National Snow and Ice Data Center (NSIDC) Distributed Active Archive Center, at the University of Colorado at Boulder [National Snow and Ice Data Center, 1998]. Monthly data were averaged over the 1978-1996 time period

to calculate monthly sea ice climatology. The climatological monthly data for August and February were used to determine the modern (maximum and minimum) extent of the seasonal ice sheet. A minimum of 5% sea ice cover was used in determining modern maximum (winter) sea ice extent. This low ice concentration was chosen to facilitate comparison with the CLIMAP (Climate: Long-Range Investigation, Mapping, and Prediction) LGM sea ice data, which did not distinguish ice concentrations, only maximum extent. A minimum of 70% ice cover was used to determine the minimum (summer) sea ice extent. Significant phytoplankton biomass can accumulate in the water column at ice concentrations below ~70% [Smith and Gordon, 1997]. Monthly sea ice data from 1997-1998 were combined with the SeaWiFS ocean color data to examine chlorophyll/phytoplankton biomass patterns within different ecological regions of the Southern Ocean. All sea ice data were remapped to a 9-km equal angle grid.

The August (maximum) LGM sea ice extent was obtained from the CLIMAP project [CLIMAP Project Members, 1976, 1981]. The data obtained from CLIMAP were on a 2° x 2° grid. Thus the spatial resolution of the CLIMAP ice extent is low. The CLIMAP sea ice boundary was remapped to a 9-km resolution equal angle grid, and the boundary was smoothed with a 50 point boxcar filter on latitude and longitude.

The mean path of the modern PF presented is from Moore et al. [1999a]. This mean path was determined by mapping the PF's position from satellite sea surface temperature data over a 7-year period, 1987-1993 [Moore et al., 1999a]. The PF marks the boundary between cold Antarctic Surface Water (ASW) to the south and warmer Subantarctic waters to the north.

We assume throughout this paper that the physiological properties of Southern Ocean phytoplankton have not changed significantly between modern and glacial times. Thus, while latitudinal range and biomass/numerical dominance within assemblages may change, the phytoplankton species present at the LGM responded to chemical and physical forcings in essentially the same way as phytoplankton in the modern day Southern Ocean. This assumption is justified because, in terms of evolutionary timescales, the LGM was a recent event.

3. Phytoplankton Biomass and Primary Production in the Modern Southern Ocean

The Southern Ocean is by far the largest HNLC region in the modern ocean [Martin, 1990]. In Plate 1, mean surface chlorophyll concentrations from the SeaWiFS satellite for the Southern Ocean during austral summer (December 1997 through February 1998) are displayed. Surface chlorophyll concentrations are indeed quite low (typically < 0.3-0.4 mg m^{-3}) despite the high concentrations of available macronutrients in the Southern Ocean (Plate 1).

The highest chlorophyll concentrations are seen in coastal waters, especially in the southern portions of the Weddell and Ross Seas and above the Patagonia shelf on the eastern coast of South America (Plate 1). Coastal waters surrounding and downstream of Southern Ocean islands also have higher chlorophyll concentrations; note the high chlorophyll values near Kerguelen Island along 70°E.

Elevated chlorophyll levels likely associated with the retreating seasonal ice cover can be seen in the Weddell Sea (in the region ~30°-0°W, 55°-67°S) and in the northern Ross Sea (~150°-170°W, 65°-75°S) [see also *Moore et al.*, 1999b].

The remaining areas of elevated chlorophyll are associated with the major fronts of the Southern Ocean. High chlorophyll values in the vicinity of the North and South Subtropical Fronts (~40°-45°S) are seen east of South America and south of Africa from ~15°-70°E (see *Belkin and Gordon* [1996] for definitions and location of the subtropical fronts). High chlorophyll levels in the vicinity of the PF can be seen in several regions, including along the Pacific-Antarctic Ridge (~145°-160°W) [see also *Moore et al.*, 1999b], approaching and crossing the Mid-Atlantic Ridge (~20°-5°W), and from ~20°-30°E (Plate 1, see Plate 4 for the mean location of the PF). There is a strong topographic influence on the dynamics of the PF in each of these regions [*Moore et al.*, 1999a]. Mesoscale physical processes may result in increased nutrient inputs to surface waters where Southern Ocean fronts interact with large topographic features [*Moore et al.*, 1999b].

In general, these patterns of chlorophyll distribution and phytoplankton biomass correlate strongly with the availability of iron for phytoplankton growth. Coastal waters including the southern Weddell and Ross Seas and near Southern Ocean islands typically have elevated dissolved iron concentrations (relative to offshore waters) in surface waters due to nearby shelf sources for iron [*Martin et al.*, 1990a, b; *Westerlund and Öhman*, 1991; *Nolting et al.*, 1991]. *Nolting et al.* [1991] found dissolved iron concentrations over the South Orkneys shelf fully an order of magnitude higher than in offshore waters. Elevated iron concentrations are also sometimes associated with melting sea ice and the Southern Ocean fronts [*Nolting et al.*, 1991; *de Baar et al.*, 1995; *Löscher et al.*, 1997; *Sedwick et al.*, 1996; *Sedwick and DiTullio*, 1997].

We can examine these patterns in chlorophyll distributions more quantitatively if we divide the Southern Ocean into ecological regions (Plate 2). We have largely followed the review of *Tréguer and Jacques* [1992] in determining these ecological boundaries. The high chlorophyll areas of the southern Weddell and Ross Seas are considered as a single region (south of 73°S, hereafter termed the Weddell-Ross Region, WRR). The WRR corresponds approximately with what *Tréguer and Jacques* [1992] termed the Coastal and Continental Shelf Zone (CCSZ). The Seasonal Ice Zone (SIZ) is defined as areas with > 5% sea ice during August 1997 and < 70% ice cover during February 1998. The Polar Front Region (PFR) is the area surrounding the PF, which we have operationally defined as the area within 1° of latitude of the mean path of the PF (see Plate 4 and *Moore et al.* [1999a]). The Permanently Open Ocean Zone (POOZ) is the region north of the SIZ and south of the PFR. The Subantarctic Water Ring (SWR) is defined as open ocean areas from the PFR north to the Subtropical Front [*Banse*, 1996]. We marked the northern boundary of the SWR as slightly north of the North Subtropical Front as defined by *Belkin and Gordon* [1996].

Not depicted in Plate 2 is the ecologically important Marginal Ice Zone (MIZ), which is a subset of the SIZ, where there has been recent melting of sea ice [*Smith and Nelson*, 1986]. The size and location of the MIZ change with the seasonal expansion and contraction of the sea ice. It is in these regions of meltwater input that phytoplankton blooms most often occur within the SIZ [*Smith and Nelson*, 1986]. We have operationally defined the MIZ as areas with > 70% sea ice cover in the preceding month and < 70% sea ice cover in the current month. A wide range of cutoff values for determining the MIZ (~30-70%) give similar results as sea ice typically melts rapidly in the Southern Ocean going from high to low concentrations in less than a month.

Note that there is some overlap between ecological regions. Near Drake Passage and in the Southwest Pacific, the SIZ overlaps with the PFR, and we have included these areas only within our MIZ and SIZ regions. Similarly, we have excluded coastal areas with depths < 500 m (shown in black in Plate 2) from the SWR, the POOZ, and the PFR to better define open ocean patterns. Areas in black near the Antarctic continent had > 70% ice cover during February 1998 and are not included in this analysis because they were heavily covered with sea ice throughout the year. Comparison with our sea ice climatology indicates that the 1997-1998 season had higher than normal summer ice cover in the Ross Sea and well below average summer ice cover in the southern Weddell Sea (see Plate 4 for the climatological February ice cover > 70%).

The seasonal chlorophyll cycles of these ecological regions as estimated with SeaWiFS are displayed in Plate 3. Note the significantly higher chlorophyll concentrations in the WRR compared with other Southern Ocean areas. The southern Weddell and Ross Seas are areas of high phytoplankton biomass and export production during austral spring and summer [*Jennings et al.*, 1984; *Smetacek et al.*, 1992; *Smith and Gordon*, 1997; *Smith and Nelson, 1990; Bates et al.*, 1998; *Arrigo et al.*, 1998]. In the southern Ross Sea, primary production often exceeds 1 g C m^{-2} d^{-1} [*Smith et al.*, 1996; *Arrigo et al.*, 1998; *Bates et al.*, 1998]. *Bates et al.* [1998] calculated mean export production at ~ 0.5 g C m^{-2} d^{-1} with an f ratio between 0.55-0.6. *Nelson et al.* [1996] calculated a seasonally integrated f ratio of 0.42. *Arrigo et al.* [1998] estimated primary production on the Ross shelf during December at 3.94 g C m^{-2} d^{-1}.

While elevated primary production is seen in the Weddell and Ross Seas, macronutrients are usually not completely depleted (nitrate concentrations typically remain > 10 μM, [e.g., *Smith et al.*, 1996]). These areas may experience some iron limitation, particularly toward the end of the summer period [*Sedwick et al.*, 1996]. *Sedwick and DiTullio* [1997] argued that a diatom bloom in the southern Ross Sea was ultimately stopped by iron limitation. *Smith et al.* [1999] also argued that micronutrient availability (notably iron) limited the growth rates of phytoplankton in the Ross Sea during late summer. Iron limitation in these areas would probably not be as severe as in offshore Southern Ocean waters due to iron inputs from sediment and melting sea ice; thus, the arguments of *Hutchins et al.* [1998] for different degrees of iron limitation in marine ecosystems likely apply in the Southern Ocean.

Lowest chlorophyll concentrations are seen in the POOZ and SWR areas with monthly mean values ranging between 0.14 and 0.32 mg m^{-3} (Plate 3). These mean values compare well with the in situ measurements compiled by *Banse* [1996]. These areas are marked by persistently high nitrate and phosphate concentrations, low chlorophyll concentrations, and low primary and export production, and
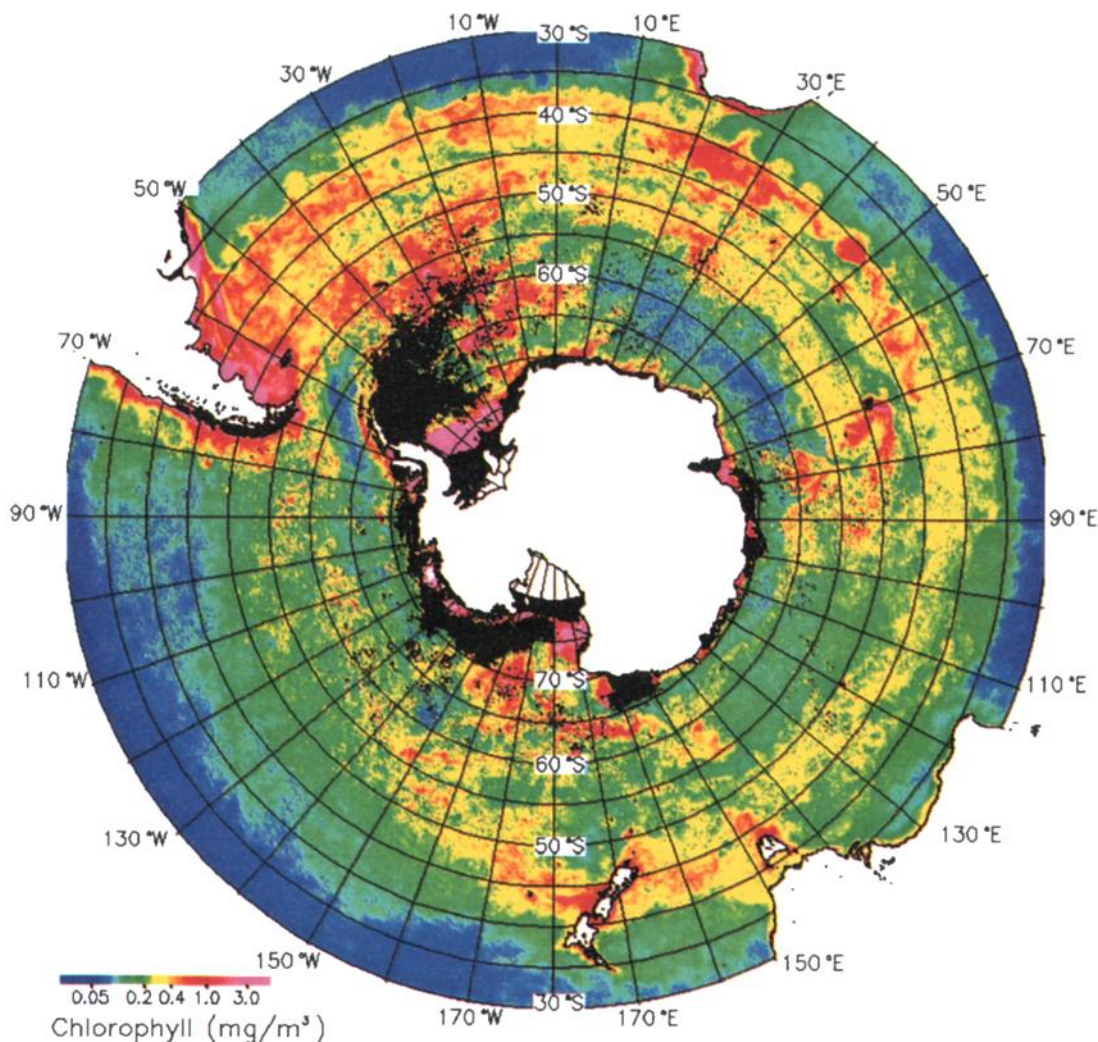
Plate 1. Shown are the mean surface chlorophyll concentrations in the Southern Ocean during austral summer (December 1997 to February 1998) from SeaWiFS.

they are dominated by smaller phytoplankton species, except in coastal waters and in the vicinity of Southern Ocean fronts [*Tréguer and Jacques*, 1992; *Banse*, 1996].

Within the SIZ there is often a short bloom dominated by large diatoms following sea ice retreat, with elevated primary and export production [*Wilson et al.*, 1986; *Nelson and Smith*, 1986; *Smith and Nelson*, 1985, 1986; *Smith and Sakshaug*, 1990]. These ice edge blooms probably account for the elevated mean chlorophyll concentrations within the MIZ and SIZ areas (Plate 3). After the initial bloom, there is typically a shift from a new production to a regenerated production regime, with a corresponding shift from larger diatoms to smaller pico-sized and nano-sized phytoplankton, similar to the POOZ and SWR pattern [*Tréguer and Jacques*, 1992; *Banse*, 1996].

Sporadic blooms of larger diatoms also occur at the PF [*Lutjeharms et al.*, 1985; *Tréguer and Jacques*, 1992; *Laubscher et al.*, 1993; *de Baar et al.*, 1995; *Banse*, 1996]. These sporadic blooms probably account for the slightly higher mean chlorophyll levels within the PFR during austral

summer (Plate 3). It should be noted that the PF is a dynamic feature, and our definition for the PFR (which is based on mean PF location) by necessity includes substantial areas that should be classified as either POOZ or SWR depending on the location of the PF. Thus chlorophyll concentrations are underestimated for the PFR, while areal extent of the area directly influenced by the front is overestimated.

The areas of these ecological regions are compared with the corresponding values from *Tréguer and Jacques* [1992] in Table 1. Differences are due to variations in the definitions of the regions and due to a different placement of the PF. *Smith and Nelson* [1986] estimated the SIZ to be ~16.4 million km^2, similar to our value despite substantially different SIZ definitions. Recall that the SIZ area in Table 1 does not include the WRR. Our estimate of the POOZ area is substantially lower than that of *Tréguer and Jacques* [1992], largely due to a different placement of the mean PF location. The SWR is by far the largest region (48.7 million km^2, Table 1). The MIZ reaches its maximum size in
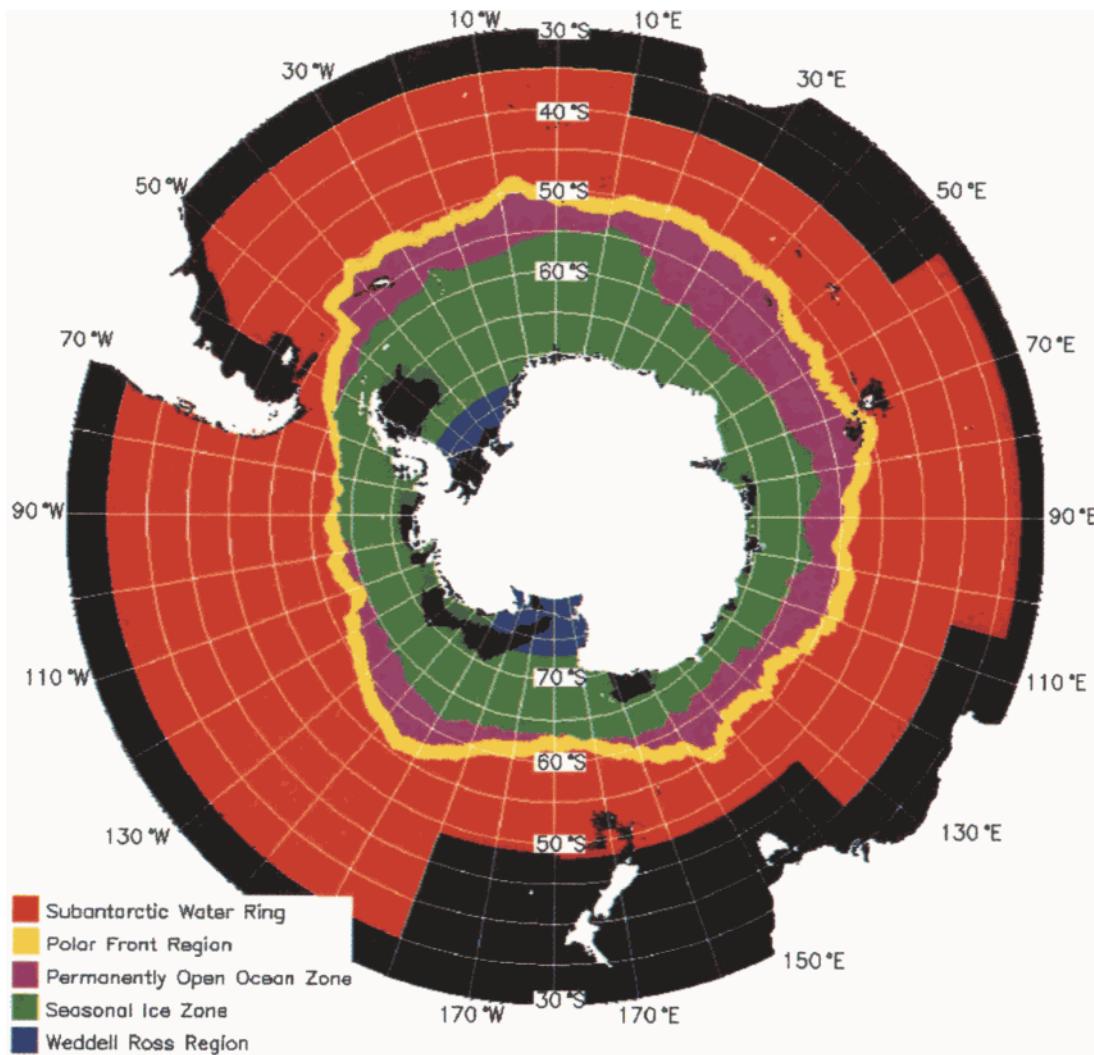
Plate 2. Displayed are ecological regions within the Southern Ocean (see text for details).

Table 1. Displayed are the Spatial Extent of Ecological Regions within the Southern Ocean for the 1997-1998 Season Compared with Values from *Tréguer and Jacques* [1992].

Region	Area	Region	Area	MIZ	Area
Subantarctic water ring	48.7			October	0.89
Polar Front region	4.89	Polar Front zone	3	November	2.82
Permanently open ocean zone	8.70	Permanently open ocean zone	14	December	6.05
				January	2.27
Seasonal ice zone	16.2	Seasonal ice zone	16	February	0.85
Weddell-Ross region	0.95	Coastal and Continental shelf	0.9	March	0.23

Column one gives the area of the ecological regions shown in Figure 2. Column 2 presents areal extent of the ecological regions of *Tréguer and Jacques* [1992]. The third column shows the area of the Marginal Ice Zone (this study)   Areas are given are in units of millions of km²
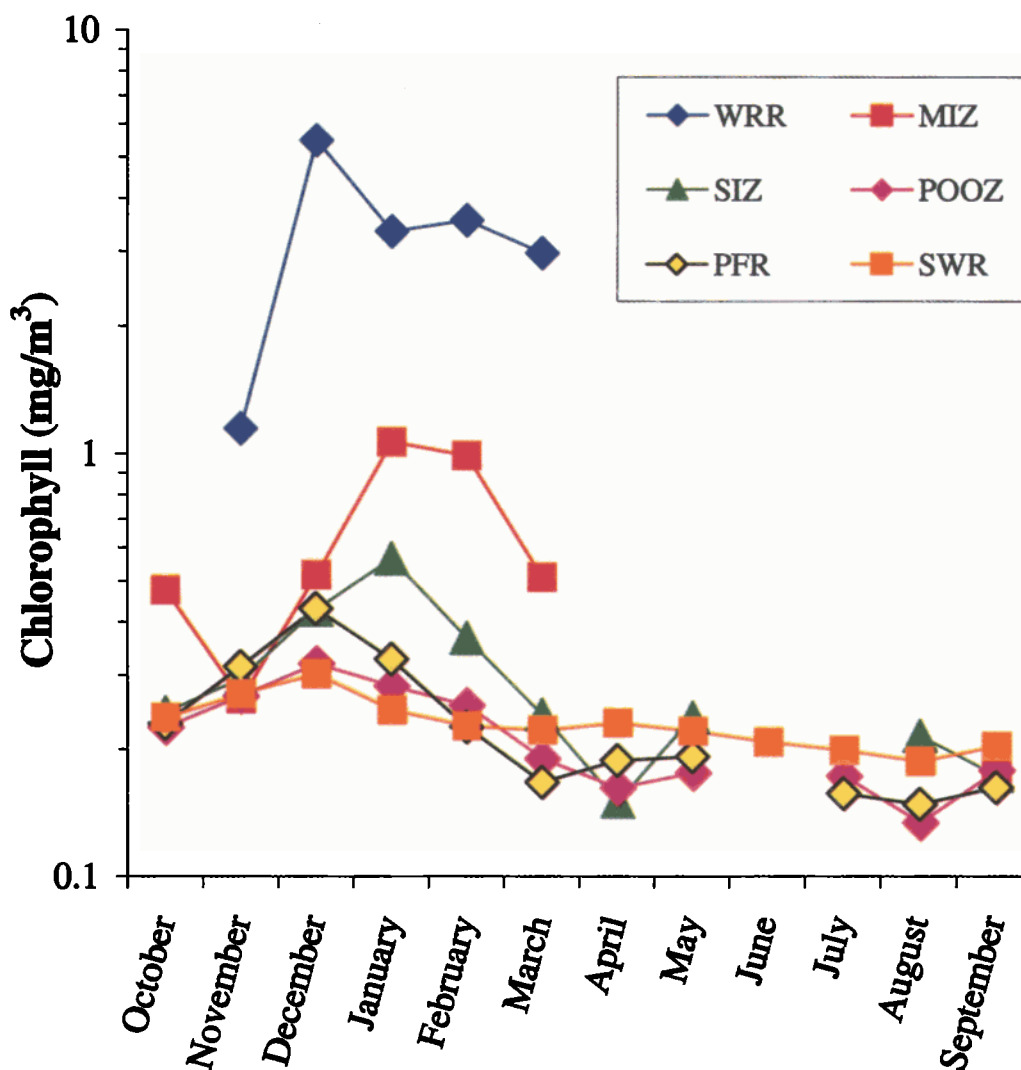
Plate 3. Shown are seasonal patterns of mean chlorophyll concentration (1997-1998) within different ecological regions of the Southern Ocean (WRR, Weddell and Ross Seas south of 73°S, SIZ, Seasonal Ice Zone, POOZ, Permanently Open Ocean Zone, PFR, Polar Front Region, MIZ, Marginal Ice Zone, and SWR, Subantarctic Water Ring). Since variability is generally low and typically thousands of data point go into each average, error bars around these means would be smaller than the symbols shown.

December, with most of its area in the Weddell Sea (Table 1).

4. Air-Sea Flux of CO_2 in the Modern Southern Ocean

The net air-sea flux of CO_2 is a function of the difference in partial pressure of CO_2 (pCO_2) between air and sea (ΔpCO_2), and the gas exchange coefficient. The gas exchange coefficient is the product of the solubility of CO_2 and the gas transfer velocity, which is a function of wind speed [Murphy et al., 1991]. The gas transfer velocity, or the rate at which gas transfers across the sea surface, is known to increase with increasing wind speed, but the exact relationship is still in question [i.e., Murphy et al., 1991]. The partial pressure of CO_2 in seawater is a function of temperature, total CO_2, total alkalinity, and salinity, with temperature and total CO_2 being the most important in surface oceanic waters [Takahashi et al., 1993].

Primary production lowers total CO_2 and pCO_2 in surface waters. The Subtropical Front has been noted as a very strong sink for atmospheric CO_2 [Metzl et al., 1991, Takahashi et al., 1993, 1997]. Takahashi et al. [1993] note that this effect is stronger in the western South Atlantic and attribute it to higher biological productivity in Subantarctic waters, combined with a cooling (lowering pCO_2) of
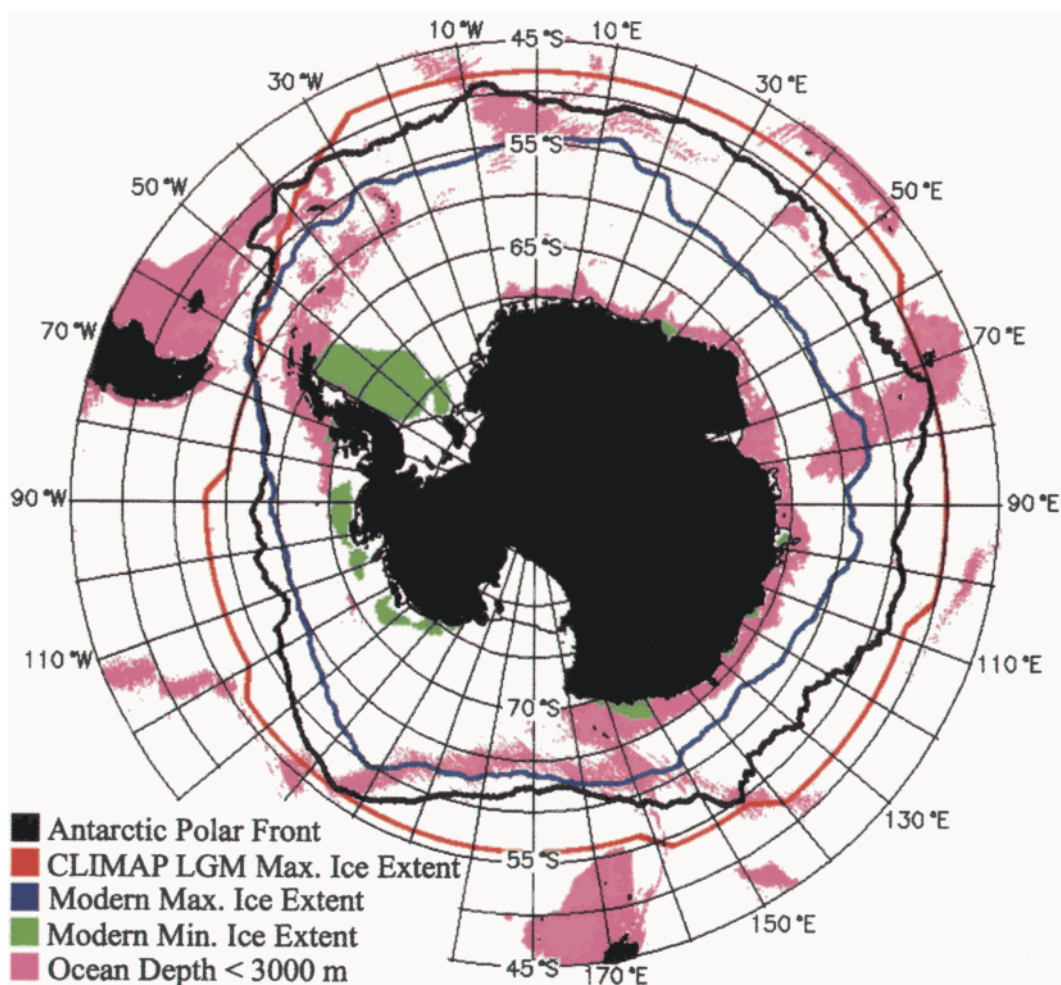
Plate 4. Shown are the maximum (August) and minimum (February) sea ice extent for the modern era from our sea ice climatology (1978-1996). Also shown is the CLIMAP project estimate of maximum ice extent at the last glacial maximum [*CLIMAP Project Members*, 1976, 1981], and the mean path of the Antarctic Polar Front [*Moore et al.*, 1999a].

Subtropical waters moving southward. The global database of ΔpCO_2 presented by *Takahashi et al.* [1997] reveals strong sinks east of Australia and Africa at these latitudes as well. In general, temperature and biota effects dominate pCO_2 in Southern Ocean waters, although in the far south the influence of salinity (i.e., from meltwater input) can also be significant [*Goyet et al.*, 1991; *Metzl et al.*, 1991, 1995; *Takahashi et al.*, 1993, 1997; *Ishii et al.*, 1998; *Sabine and Key*, 1998].

Net air-sea CO_2 fluxes south of the PF are controlled largely by the biota and mixing processes, as seasonal temperature effects are relatively small. Much of this region is a weak net source or sink of CO_2 for the atmosphere in the modern Southern Ocean [*Murphy et al.*, 1991; *Robertson and Watson*, 1995; *Bakker et al.*, 1997; *Takahashi et al.*, 1997]. Relatively carbon-rich waters upwell at the Antarctic Divergence (AD) and enter surface waters through vertical

mixing. The balance between this carbon source and photosynthetic production largely determines the direction of the net air-sea flux of CO_2 in Antarctic surface waters during the austral growing season. Areas of high primary production are strong sinks for atmospheric CO_2, while areas of low production are typically regions of low net flux, which can be in either direction [*Bouquegneau et al.*, 1992; *Metzl et al.*, 1991, 1995; *Takahashi et al.*, 1993, 1997; *Rubin et al.*, 1994; *Poisson et al.*, 1994; *Robertson and Watson*, 1995; *Ishii and Sugimura*, 1998; *Bates et al.*, 1998; *Inoue et al.*, 1998].

The southern Weddell and Ross Seas become strong sinks for atmospheric CO_2 during summer, due to high biological production [*Takahashi et al.*, 1993, 1997; *Bates et al.*, 1998]. *Bates et al.* [1998] found pCO_2 values ranging from 50-150 μatm (mean ~100 μatm) below atmospheric levels along 76 5°S in the Ross Sea during austral summer

Estimated CO_2 flux into the ocean ranged from 4-26 mmol C m^{-2} d^{-1} [*Bates et al.*, 1998]. They suggested that this area was an annual net sink for atmospheric CO_2 due to strong biological production during austral summer and little net flux the rest of the year because of persistent ice cover [*Bates et al.*, 1998].

Along 6°W in the austral spring of 1992, the PF was a strong sink for atmospheric CO_2 (due to phytoplankton production), while most of the area farther south was a net source (due to the seasonal warming of surface waters and very low phytoplankton production) [*Bakker et al.*, 1997]. Thus the seasonal temperature effect on pCO_2 can be significant for net air-sea flux in areas of very low phytoplankton biomass/production.

5. Sea Ice at the LGM

5.1. Winter Sea Ice Extent at the LGM

The maximum sea ice extent at the LGM covered a much larger area than it does in the modern ocean [*CLIMAP Project Members*, 1976, 1981; *Cooke and Hays*, 1982; *Crosta et al.*, 1998a]. The estimated maximum LGM sea ice extent from the CLIMAP project is shown in Plate 4 [*CLIMAP Project Members*, 1976, 1981]. Plate 4 also shows the mean location of the modern-day PF and the maximum and minimum sea ice extent in the modern Southern Ocean. Several studies have arrived at similar boundaries for maximum sea ice extent at the LGM [*Hays et al.*, 1976; *Cooke and Hays*, 1982; *Crosta et al.*, 1998a] (see *Crosta et al.* [1998a] for a comparison of these ice extent boundaries). *Crosta et al.* [1998a] based their estimate on the presence of ice-associated species of diatoms in the sediment. They argued that the maximum extent of sea ice was several degrees of latitude farther north than the CLIMAP position in the southwest Atlantic and several degrees farther south than the CLIMAP estimate in the southeast Pacific [*Crosta et al.*, 1998a]. Very few sediment cores from the Pacific sector of the Southern Ocean were used in constructing the CLIMAP boundary. In section 6 we argue that the CLIMAP winter ice boundary is placed too far north over much of the Pacific sector.

A number of factors could have contributed to this ice age expansion of the seasonal ice sheet. Cooler atmospheric and sea surface temperatures would promote ice formation [*Martinson*, 1990; *Crosta et al.*, 1998b]. A decrease in the input of warm salty North Atlantic Deep Water (NADW) to the ACC during glacial times has also been suggested to play a role [i.e., *Crowley and Parkinson*, 1988]. Wind-driven advection was probably an important factor. The increased wind speeds of the LGM [*Petit et al.*, 1981] would advect ice formed in southern regions farther north at the LGM; the resulting leads (openings within the pack ice) would rapidly freeze over due to the cold atmospheric temperatures [*Smith et al.*, 1990]. *Cavalieri and Parkinson* [1981] suggested a strong atmospheric cyclonic low pressure system led to rapid sea ice expansion in the Weddell Sea by moving cold air and sea ice equatorward. *Comiso and Gordon* [1998] found maximum winter ice extent in the Weddell Sea to be positively correlated with meridional wind speeds.

5.2. Summer Sea Ice Extent at the LGM

Several studies have suggested a greatly expanded summer sea ice extent at the LGM, well north of the maximum winter ice extent of today [*CLIMAP*, 1981; *Hays et al.*, 1976; *Cooke and Hays*, 1982]. This boundary is only ~2°-5° of latitude south of the CLIMAP winter sea ice boundary shown in Plate 4. The CLIMAP summer ice boundary was drawn along the sedimentary boundary between diatom ooze to the north and diatomaceous clay to the south. Burckle and coworkers showed that this sedimentary boundary does not mark minimum ice extent in the modern ocean and that the CLIMAP LGM summer ice boundary did not mark minimum extent, but rather a late spring/early summer sea ice extent, slightly north of the modern mid-December position [*Burckle et al.*, 1982; *Burckle*, 1984; *Burckle and Cirilli*, 1987]. *Burckle and Cirilli* [1987] noted that waters south of this ice edge experience only a few months of ice-free time each year, resulting in a depressed annual flux of diatoms to the sediments that results in the silty, diatomaceous clay sediment type.

Crosta et al. [1998b] combined a detailed study of modern and LGM diatom species distributions in the sediment to estimate summer sea ice cover. They noted the presence of open ocean diatom species in all of their LGM sediment samples, indicating at least some ice-free time each summer [*Crosta et al.*, 1998b]. The data presented by *Crosta et al.* [1998b] argue strongly that summer sea ice extent was south of 60°S in the Atlantic and Indian sectors and south of 65°S in the Pacific. They concluded that summer sea ice extent at the LGM was very similar to today's minimum sea ice extent, south of all their core locations [*Crosta et al.*, 1998b]. Therefore, for the purposes of this paper, we will assume that the minimum (summer) sea ice extent at the LGM was the same as in the modern Southern Ocean. This assumption represents a current best guess of summer ice extent at the LGM. *Crosta et al.* [1998b] examined few cores from the southwest Pacific sector and none from the Weddell and Ross Seas. There is evidence that summer sea ice extent in the Weddell Sea was somewhat greater than in the modern era [*Jordon and Pudsey*, 1992; *Shimmield et al.*, 1994]. In addition much of the Ross Sea shelf was covered by grounded ice sheets at the LGM [*Kellogg*, 1987; *DeMaster et al.*, 1996]. The SIZ at the LGM was thus much larger than in the modern era, due to a greatly expanded winter sea ice area and summer ice cover similar to today.

A summer sea ice distribution at the LGM similar to today's seems counterintuitive, given the colder atmospheric and sea surface temperatures. However, much of the heat required for seasonal melting of the pack ice comes from the relatively warm Circumpolar Deep Water below the surface layer through upwelling at the AD and vertical mixing [*Gordon*, 1981]. *Comiso and Gordon* [1996] attributed the persistent formation of the Cosmonaut polynya during austral winter to the upwelling of warmer subsurface waters. Enhanced advection due to the increased mean wind speeds also probably played an important role, as ice advected northward into open ocean would melt more rapidly than in heavy ice covered areas [*Martinson*, 1990]. Likewise increased lead and polynya formation due to wind advection would enhance ice melting in spring, as these open water areas absorb solar radiation more efficiently than ice-covered

areas due to their lower albedo [*Smith et al.*, 1990]. *Comiso and Gordon* [1998] found that unusually low summer sea ice extents in the Weddell Sea follow winters with higher than normal sea ice extent. They attributed this surprising phenomenon to a combination of wind effects including increased northward advection of sea ice [*Comiso and Gordon*, 1998].

5.3. Sea Ice Seasonality

The greatly expanded SIZ of the last glacial period has profound implications for Southern Ocean ecology and air-sea fluxes of CO_2. The spring ice retreat during glacial times would have begun later in the season and much farther to the north, because of the cooler atmospheric temperatures and expanded winter ice cover. Likewise the fall ice expansion would have begun earlier in the season. Indeed, the CLIMAP summer ice boundary and the boundary of *Cooke and Hays* [1982], which likely record the late spring/early summer (approximately mid-December) ice extent, are well north of today's maximum winter sea ice extent [*CLIMAP*, 1981; *Cooke and Hays*, 1982; *Burckle et al.* 1982; *Burckle*, 1984]. This indicates a substantial delay in the seasonal retreat of the pack ice at the LGM.

Primary production beneath heavy pack ice is negligible due to the poor transmission of light through snow and ice [*Fischer et al.*, 1988; *Wefer and Fischer*, 1991; *Bouquegneau et al.*, 1992]. Thus, the effective growing season for phytoplankton south of the PF was shorter at the LGM, with progressively decreased ice-free time as one moved poleward [*Burckle and Cirilli*, 1987; *Crosta et al.*, 1998b]. *Crosta et al.* [1998a] estimated months of sea ice cover per year at the LGM based on diatom species assemblages in the sediments. They estimated that in areas north of the modern-day maximum ice extent there was ~3-5 months per year of substantial sea ice cover in the Atlantic Sector and 1-2 months in the Indian Sector at the LGM [*Crosta et al.*, 1998a]. If the CLIMAP summer ice boundary does mark a mid-December ice extent, these estimates would seem to underestimate the duration of seasonal ice cover. *Crosta et al.* [1998a] note that their low values in the Indian sector are likely underestimates due to advection and focusing of sediments or perhaps due to diatom frustule dissolution within the sediments. Thus, within the expanded SIZ, the effective growing season for phytoplankton at the LGM was much reduced relative to the modern ocean, perhaps by 50% or more in areas north of the modern maximum ice extent.

5.4. Physical Effects of the Expanded Seasonal Ice Zone on Air-Sea CO_2 Fluxes

Expanded seasonal ice cover would reduce the outgassing of CO_2 to the atmosphere during winter months by acting as a barrier to air-sea exchange as happens today in the Weddell Sea during winter [*Weiss*, 1987; *Bakker et al.*, 1997; *Crosta et al.*, 1998a]. This barrier effect can lead to supersaturation of CO_2 beneath heavy ice cover. The accumulated CO_2 may not outgas during the spring ice melt because the input of meltwater lowers TCO_2 and pCO_2 in surface waters and spring phytoplankton production also decreases pCO_2 [*Hoppema et al.*, 1995; *Ishii et al.*, 1998; *Sabine and Key*, 1998].

Persistent ice cover over the AD could also have slowed Ekman upwelling during winter months and, thus, reduced nutrient and carbon inputs to the surface layer. Ice would still advect away from the AD, and new ice would form rapidly in the leads owing to the very cold air temperatures. However, some of the wind momentum imparted to surface waters in the modern Southern Ocean (where the AD is ice-free much of the year) would be absorbed by sea ice at the LGM. *Wamser and Martinson* [1993] concluded that typical winter pack ice cover in the Weddell Sea reduces the momentum flux from the atmosphere to the ocean by ~33%. The momentum flux from atmosphere to ocean is little affected by thin ice or at low ice concentrations, so any reduction in upwelling would be restricted to winter months. This postulated reduction in upwelling might also be counterbalanced to some extent by the increased mean wind speeds (and thus northward advection) at the LGM [*Petit et al.*, 1981].

6. Sea Ice and the Antarctic Polar Front

6.1. The Antarctic Polar Front as a Boundary for Sea Ice Extent

Through much of the Drake Passage region, the maximum extent of sea ice in the modern ocean is coincident with the mean location of the PF (Plate 4). The warmer sea surface temperatures in Subantarctic Surface Waters north of the PF rapidly melt sea ice entering the front. For this reason, there is sometimes a pulse of ice-rafted debris at the PF [*Watkins et al.*, 1982]. The location of the PF thus sets the maximum extent of the seasonal sea ice cover in this area of the Southern Ocean today. Similarly, in the southwest Pacific (~ 175°E), the PF also likely restricts the maximum extent of sea ice (Plate 4). While SST values were lower at the LGM, Subantarctic waters north of the PF were still above the freezing point of seawater [*CLIMAP*, 1976, 1981] and would thus rapidly melt sea ice in areas north of the PF. We suggest that the PF marked the maximum extent of the seasonal sea ice over the entire Southern Ocean at the LGM (Plate 4).

The CLIMAP sea ice boundary is north of the present mean location of the PF in many areas (Plate 4). However, it is within the latitudinal range of meanders of the PF over almost the entire Southern Ocean [*Moore et al.*, 1999a]. Only in the southwest Pacific near 180°W and in the southeast Pacific around 100°W is the CLIMAP boundary north of the envelope of PF paths documented by *Moore et al.* [1999a]. It is also in these areas that the CLIMAP boundary is most suspect due to a paucity of sediment cores. *Cooke and Hays* [1982] place the maximum ice extent ~5° latitude farther south along 180°W based on ice-rafted debris distributions in the sediments. Thus the CLIMAP maximum ice extent could be recorded in the sediments without transport of ice north of the PF or a northward migration of the PF mean location.

6.2. A Glacial Northward Shift of the Antarctic Polar Front?

A number of authors have suggested that the PF was shifted northward as much as 10° of latitude during the last ice age, possibly due to a similar shift in the winds [*Climap*

Project Members, 1976; *Hays*, 1978; *Dow*, 1978; *Prell et al.*, 1980; *Defelice and Wise*, 1981; *Morley*, 1989; *Howard and Prell*, 1992; see also *Klinck and Smith*, 1993]. These papers relate modern-day species assemblages in the sediments (typically diatoms, radiolaria, or foraminifera are used) to current SST and water mass distributions then estimate past SST and frontal locations using the modern analogs. A crucial assumption, either implicit or explicit, of all of these studies is that the PF retains its role as an ecological boundary over glacial/interglacial timescales. Thus if a predominantly "polar" assemblage (an assemblage found south of the PF today) is found farther north in sediments from the LGM, it is assumed that the PF has shifted northward.

This interpretation overlooks the possibility that today's polar assemblages may have extended their range north of the PF during glacial periods. We suggest that while surface isotherms (and polar biota assemblages) shift equatorward during glacial periods, the location of the PF, which is tightly controlled by topography, remains unchanged. There was still a strong gradient in surface temperatures across the PF during glacial times, but waters north and south of the front were colder. The PF marks the boundary between cool, fresh Antarctic Surface Water to the south and warmer, saltier Subantarctic Surface Water to the north. However, it is not tied to a particular isotherm. In fact there is considerable regional and latitudinal variability in mean SST values at the poleward edge of the PF within the modern Southern Ocean [*Moore et al.*, 1999a]. Thus the PF today is a physical water mass boundary and an ecological boundary. However, the two likely became uncoupled at the LGM with the ecological boundary between polar and subpolar species shifting north of the PF.

The PF today forms an ecological boundary primarily due to the change in SST across the front. Subantarctic waters north of the PF reach much warmer temperatures during summer than the cooler Antarctic Surface Waters to the south. Some nutrients, notably silica, can have strong cross-frontal gradients that may also influence species composition. The much cooler SST values in Subantarctic waters at the LGM (~3°-6°C colder at the LGM [*Pichon et al.*, 1992; *Nelson et al.*, 1993; *Ikehara et al.*, 1997]) may have allowed today's polar species to thrive in Subantarctic waters. *Burckle* [1984] argued that the northern limit of high productivity by diatoms is controlled by a temperature effect on the metabolic processes of diatoms. *Neori and Holm-Hansen* [1982] found that the photosynthetic rates of Antarctic diatoms dropped off sharply at SST values above 7°C. *Fiala and Oriol* [1990] found that Antarctic diatoms could not survive in temperatures above 6-9°C. Thus the cooler SST values at the LGM may have allowed Antarctic diatoms to extend their latitudinal range equatorward. Silica concentrations may also limit diatom growth in Subantarctic and northern Antarctic Surface Waters [*Tréguer and Jacques*, 1992]. Under iron-replete conditions, silicic acid requirements decline relative to nitrate [*Hutchins and Bruland*, 1998; *Hutchins et al.*, 1998; *Takeda*, 1998]. *Hutchins et al.* [1998] found that under iron-limitation diatoms were more highly silicified than under iron-replete conditions. Thus the increased atmospheric flux of iron may also have promoted diatom production in Subantarctic waters by lowering cellular silica quotas.

Labeyrie et al. [1996], studying a sediment core from ~96°E, 46°S, estimated glacial summer SST values of ~2.0°-

2.5°C using a diatom transfer function. These SST values are similar to those found south of the PF today (mean summer SST at the poleward edge of the PF is ~2.8°C [*Moore et al.*, 1999a]). Yet *Labeyrie et al.* [1996] noted that the low instance of the "ice-related" factor in this core indicates that it was always north of the PF. *Weaver et al.* [1998] note the replacement of "subpolar" by "polar" assemblages of Foraminifera in Subantarctic waters during glacial times. SST values north and south of the PF were cooler at the LGM [*Pichon et al.*, 1992]; thus estimates of LGM SST based on species assemblages are likely accurate, but no northward migration of the PF is required to account for these SST/species assemblage shifts.

The warmer, saltier Subantarctic waters found north of the PF would rapidly melt sea ice in modern and glacial times. Thus estimates of maximum sea ice extent may mark the LGM PF location better than analogs of modern species assemblages. However, as noted previously, estimates of maximum sea ice extent are consistent with little or no northward migration of the PF. The maximum ice extent of *Cooke and Hays* [1982] (based on ice-rafted debris) is virtually identical to their position for the modern day PF, except in the Atlantic sector, where the ice extends ~1°-2° farther north. This is consistent with little or no northward migration of the PF as meanders of the front could bring sea ice north of the mean position.

The PF extends from the sea surface to the ocean floor, and, thus, its location is strongly influenced by bottom topography [*Deacon*, 1937; *Moore et al.*, 1997; 1999a]. For this reason, the winds can only indirectly affect the location of the PF. In several areas of the Southern Ocean, the location of the PF is tightly controlled by the topography [*Moore et al.*, 1997, 1999a]. In these areas of strong topographic control, a northward migration of the PF at the LGM is unlikely. Strong topographic control of the PF occurs through much of the Drake Passage region, along the eastern flank of Kerguelen Plateau (~75°E), and where the PF crosses the Pacific-Antarctic (~145°W), the Mid-Atlantic (~8°W), and Southeast Indian Ridges (~145°E) [*Moore et al.*, 1997, 1999a]. In each of these areas the CLIMAP LGM maximum sea ice extent is at or close to the present location of the PF (Plate 4). This indicates strongly that the PF did not migrate northward in these areas, especially when the low spatial resolution of the CLIMAP data set is considered. *Moore et al.* [1999a] showed that seasonal and interannual variability in the location of the PF is negligible in these areas of strong topographic control; thus, variations in wind forcing over these timescales have no effect on the location of the front.

Away from large topographic features, above the deep ocean basins, the PF is able to meander over a broader latitudinal range [*Moore et al.*, 1999a]. In these areas, a northward shift in the mean location of the PF is perhaps possible. Interannual and seasonal variability is higher in these areas, but temporal coverage is poor [*Moore et al.*, 1999a]. Thus it is difficult to say whether the mean path shifts over interannual timescales or is merely not well resolved. It is in these areas that the CLIMAP ice extent boundary is farthest north of the modern PF location (e.g., ~110°-90°W, ~80°-140°E, in Plate 4).

Thus the PF likely delimited the northward extent of the SIZ throughout the Southern Ocean at the LGM (Plate 4). We suggest that on average, the maximum sea ice extent

at the LGM was ~1° north of the mean location of the PF depicted in Plate 4. In the areas with strong topographic control on the PF discussed above, maximum ice extent could not be very far north of the mean PF position (as happens today in Drake Passage). In areas where the PF meanders more extensively, northward meanders could allow sea ice to reach areas several degrees of latitude north of the mean PF location. In the modern Southern Ocean, the PF meanders over a latitudinal range that typically spans between 2° and 5° of latitude [Moore et al., 1997, 1999a].

Estimates of sea ice cover in the modern ocean and at the LGM are summarized in Table 2. We calculated the maximum ice extent at the LGM as 1° north of the modern day mean PF position. Thus the LGM SIZ encompasses the PFR, POOZ, SIZ, and WRR regions of the modern Southern Ocean (see Table 1). Recall that for Table 1 we used sea ice extent from the 1997-1998 season in calculating regional area, while in Table 2 we have used the climatological ice cover from the years 1978-1996. The LGM sea ice distribution is quite different from the modern ocean. The POOZ covers ~9.7 million km² in the modern Southern Ocean but did not exist at the LGM (Table 2). The SIZ was thus much larger in the glacial Southern Ocean, covering ~30 million km², compared with ~19 million km² which we calculate as the size of the SIZ today (Table 2).

The ocean area south of our smoothed CLIMAP maximum ice extent (Plate 4), covers 37.5 million km². We suggest that the sparse core data used by the CLIMAP project overestimated maximum ice extent in some regions, notably in the Pacific Sector, where few cores were available and the CLIMAP boundary is well north of the PF (Plate 4). Over most of the Southern Ocean our estimate of maximum ice extent based on PF location is in rough agreement with previous estimates based on the geological record. Gloersen et al. [1992] calculated modern maximum ice extent (all ice concentrations) as 19 million km² with some 3.5 million km² of open water within this region. Likewise they calculated summer ice cover as ~4-4.5 million km², which includes some 1.5 million km² of open water and substantial areas with < 70% ice cover [Gloersen et al., 1992].

7. Southern Ocean Ecology at the LGM

7.1. Antarctic Coastal Waters

Much of what constitutes coastal Antarctic waters in today's ocean was either above sea level or beneath grounded ice sheets at the LGM [Kellogg, 1987]. This would lead to lower primary production in coastal regions. Mackensen et al. [1994] suggested reduced productivity along the continental margin at the LGM based on sediment δ C data. Due to the small areal extent of coastal waters, this would have little effect on the total productivity of the Southern Ocean [Arrigo et al., 1998]. However, any reduction in the productivity of coastal waters could have had dire consequences for higher trophic levels that depend on these areas for foraging, such as the Adelie penguins, which reproduce only on the Antarctic continent [Nicol and Allison, 1997]. The fact that these shore-breeding birds survived the last ice age is evidence for substantial high-productivity open water near the Antarctic continent during austral summer at the LGM, likely owing to a strong summertime retreat of the seasonal ice sheet as proposed by Crosta et al. [1998b]. Persistent, large coastal polynyas could also have provided suitable foraging grounds.

7.2. The Seasonal Ice Zone - From the Antarctic Polar Front to the Antarctic Continent

Much of the primary production in the modern SIZ occurs during a short (several weeks), intense phytoplankton bloom following the retreat of the seasonal ice cover [Smith and Nelson, 1986; Tréguer and Jacques, 1992]. Macronutrients are typically not completely used up in ice edge blooms today [Jennings et al., 1984; Nelson and Smith, 1986; Smith and Sakshaug, 1990]. Iron availability may ultimately limit macronutrient drawdown [Sedwick and DiTullio, 1997]. Thus the increased aeolian iron fluxes at

Table 2. Areal Extent of Sea Ice Coverage and Ecological Regions in the Modern Southern Ocean and at the Last Glacial Maximum.

	Modern Southern Ocean	LGM Southern Ocean
Winter maximum ice extent	20.1	31.0
Summer minimum ice extent	1.2	1.2
Seasonal ice zone	18.9	29.8
Permanently open ocean zone	9.7	0.0

Modern day winter sea ice extent was calculated as areas with > 5% sea ice cover during the month of August in our sea ice climatology (1978-1996). Winter sea ice extent at the LGM is estimated to extend on average 1 degree of latitude north of the mean location of the Antarctic Polar Front as defined by [Moore et al., 1999a]. Modern summer sea ice extent is calculated as areas with > 70% sea ice cover during February in our sea ice climatology. LGM summer sea ice extent is assumed identical to the modern era, based on the data of Crosta et al. [1998b]. The Permanently Open Ocean Zone (POOZ) is calculated as the area south of the mean position of the Antarctic Polar Front [Moore et al., 1999a] with < 5% ice cover during August in our sea ice climatology. The Seasonal Ice Zone (SIZ) is calculated as the difference in area between the winter maximum and the summer minimum ice extent. All values given are millions of km².

the LGM probably led to more intense spring blooms of phytoplankton following the retreating ice edge. The greatly expanded size of the SIZ at the LGM also means that ice edge blooms would have occurred over a much larger area than in the modern ocean. In addition, the elevated ice age aeolian dust flux may have allowed larger diatoms to bloom within the SIZ throughout the austral growing season, without the postbloom species shift toward smaller phytoplankton species (with lower export production) often seen today. As noted previously, this is basically the pattern observed in the southern Weddell and Ross Seas today.

Sedimentary estimates of paleoproductivity for the area south of the PF tend to indicate lower export production at the LGM compared with the modern era [Mortlock et al., 1991; Charles et al., 1991; Shemesh et al., 1993; Shimmield et al., 1994; Kumar et al., 1995]. Francois et al. [1997] found export fluxes in the eastern Indian sector were similar to modern values. As previously mentioned, paleoproductivity estimates that rely on biogenic opal are probably too low because of changing C/Si ratios over glacial-interglacial timescales [Takeda, 1998].

Bottom current redistribution of sediments must also be taken into account, and normalizing opal flux to excess ^{230}Th activity can correct for this resuspension problem [Francois et al., 1997]. For example, Charles et al. [1991] and Mortlock et al. [1991] argued for lower glacial productivity in core RC13-271 located just south of the PF (51°59'S, 04°31'E). Kumar et al. [1995] showed evidence of increased particle and organic carbon flux at this site during the LGM based upon different paleoproxies with the Th flux correction. Anderson et al. [1998] documented higher organic carbon accumulation at the LGM in this core relative to the Holocene.

The cores farthest south of the PF seem to show the greatest LGM reduction in flux to the sediments [Charles et al., 1991; Mortlock et al., 1991; Shimmield et al., 1994; Kumar et al., 1995; Anderson et al., 1998]. This is consistent with increased winter ice cover (shorter growing season) at higher latitudes [Burckle, 1984; Charles et al., 1991; Shimmield et al., 1994]. All of the cores in these studies (except for Shimmield et al. [1994]) are north of the maximum ice extent of today's Southern Ocean (Plate 4). Thus the growing season for phytoplankton at the LGM was much shorter, as these regions were likely ice-covered for much of the year. This raises the possibility that while annual fluxes to the sediments may have been lower at the LGM, primary production and export fluxes over daily to monthly timescales may have been similar or increased relative to the modern Southern Ocean.

There is evidence for this hypothesis of increased spring/summer primary production at the LGM. In their analysis of core RC13-271 (51°59'S, 04°31'E), Anderson et al. [1998] compared mean Holocene and LGM opal and organic carbon (C-org) accumulation rates. Rates of opal accumulation were similar (123 mmol m^{-2} yr^{-1} for the Holocene and 117 mmol m^{-2} yr^{-1} for the LGM), but the accumulation of organic carbon was substantially higher at the LGM (5.56 mmol m^{-2}yr^{-1} LGM, and 3.77 mmol m^{-2}yr^{-1} Holocene) [Anderson et al., 1998]. This site is slightly south of the PF and north of the maximum ice extent today but was ice covered much of the year at the LGM (Plate 4). Thus despite the shorter effective growing season, the annual organic C flux increased. Four other cores south of 50°S in this region had higher accumulations of authigenic U at the LGM, also implying higher fluxes of organic carbon to the

sediments [Anderson et al., 1998]. Farther south at core RC13-259, organic carbon accumulation was lower at the LGM by nearly 50% [Anderson et al., 1998]. High accumulation rates of ice-rafted debris in this core indicate substantial ice cover at the LGM [Cooke and Hays, 1982]. Thus if the growing season was reduced by 50%, the carbon accumulation data would argue that daily export fluxes did not change between the LGM and the Holocene at this core location, while the other cores just to the north had increased export production at the LGM. The ecological regime shift at the LGM suggested here (with increased production by larger phytoplankton species) could have resulted in a more efficient transport of organic carbon to the deep ocean as larger cells (especially diatoms) sink faster than small cells.

Further support for this hypothesis can be found in the data of Francois et al. [1997], who analyzed the bulk δ N signal in modern and glacial age sediments and found consistently higher values south of the PF at the LGM. This indicates more efficient nitrate utilization at the LGM (~70%) than in the modern Southern Ocean (~30% [Francois et al., 1997]). Francois et al. [1997] also noted that annual export production (as measured by excess^{231}Pa$_0$/excess^{230}Th$_0$ particle flux method) and preserved opal flux to the sediments declined (South Atlantic and central Indian Ocean) or remained at similar levels to modern values (East Indian sector). Export fluxes were similar over most of the region south of the PF (averages south of PF of 0.13 (Holocene) and 0.14 (LGM) for excess^{231}Pa$_0$/excess^{230}Th$_0$, and a range of 0.4-1.0 preserved ^{230}Th-normalized opal fluxes in cm^{-2} kyr^{-1} during both periods [Francois et al., 1997, Figure 1]).

From these two facts, increased nitrate utilization and a similar or lower annual export flux, Francois et al. [1997] concluded that nutrient inputs to the surface layer must have been much lower during the LGM, which they attributed to increased vertical stratification of the water column. They estimated that nutrient input to the surface layer would have to have been 10 times lower at the LGM due to increased stratification (water supply by vertical mixing and upwelling of ~30 m yr^{-1} for the Holocene and ~3 m yr^{-1} at the LGM [Francois et al., 1997]). This represents a drastic decrease in nutrient inputs relative to the modern era. Hoppema et al. [1995], for example, estimated entrainment rates in the Weddell Sea today of 4-5 m month^{-1}, and Gordon and Huber [1990] estimated upwelling rates of Weddell Deep Water at 45 m yr^{-1}. These two estimates come from areas where the influence of the seasonal ice cover is very strong.

We suggest an alternate interpretation of the data presented by Francois et al. [1997] that does not require a large reduction in nutrient inputs to the surface layer. Nearly all of the cores analyzed in their study are north of the maximum sea ice extent of today and south of the maximum ice extent at the LGM (Plate 4). In the modern Southern Ocean, these regions are marked by low phytoplankton biomass and low export production over a 12 month growing season. Thus nitrate concentrations remain high, and the sediment δ^{15}N data indicate low nitrate utilization. At the LGM, the effective (ice-free) growing season was much shorter, with perhaps only 3-6 months of production per year. Relatively short, intense phytoplankton blooms stimulated by the sea ice retreat and increased atmospheric iron deposition would have resulted in much more efficient utilization of surface nitrate (as happens in coastal and ice edge blooms in the modern Southern Ocean). This could explain the results presented by Francois et al. [1997] without decreasing nutrient inputs to the surface layer at the LGM.

The large reduction in annual nutrient inputs to the surface layer due to increased water column stratification proposed by Francois et al. [1997] appears at variance with other observations. An increase in water column stratification would have to be salinity driven and would be controlled largely by the balance between ice formation and melting, as the cooler sea surface temperatures of the LGM would tend to destabilize the water column. Areas with high input of meltwater during austral spring would become more stratified, but this effect would be restricted to a relatively short period. In these northern areas where ice melting exceeded ice formation, the strong winds over the Southern Ocean would erode any meltwater-induced stability by the following fall (as happens in the SIZ today), when deep mixing (and thus high nutrient injection) would occur. Several authors have suggested open ocean deep convection at the LGM due to a decrease in the stratification of surface waters [Martinson, 1990; Rosenthal et al., 1997]. Areas farther south near the AD, where much of the seasonal pack ice is formed, would be less stratified due to increased brine injection during ice formation. Much of the nutrient input to Southern Ocean surface waters occurs at the AD, and the higher mean wind speeds [Petit et al., 1981] and increased brine input argue that the upwelling rate and nutrient input was likely higher at the LGM (at least during austral summer). Thus the large increase in stratification necessary to account for the ~10 fold reduction in nutrient input over annual timescales suggested by Francois et al. [1997] is unlikely. The proposed stratification increase and corresponding reduction in CO_2 outgassing would have occurred only seasonally during the spring ice melt.

In contrast, current understanding of the role of iron in Southern Ocean ecosystems argues strongly that the combined influence of meltwater input and elevated aeolian dust flux would have led to higher primary production and export fluxes during austral spring and summer. It could be argued that the higher wind speeds would deepen mixed layers, leading to light limitation and thus preventing production increases during summer. However, the high nitrate utilization efficiencies reported by Francois et al. [1997] argue that this did not happen. In addition, because light harvesting efficiency is greater in iron-replete cells [Sunda and Huntsman, 1997], the increased iron flux from the atmosphere during the last ice age may have improved the photosynthetic efficiencies of Antarctic phytoplankton at low light levels, allowing them to adapt to any deepening of mixed layers.

7.3. Primary Production and DMS Release by Phaeocystis at the LGM

Shifts in species composition could also complicate the picture south of the PF. As pointed out by Martin [1990], Phaeocystis spp. are common phytoplankton in Antarctic coastal waters and may have increased their abundance and range at the LGM. These phytoplankton contain no hard parts (i.e., opal, $CaCO_3$) and would likely leave little in the way of a sedimentary signal [Martin, 1990]. Phaeocystis has a complex life cycle, alternating from a colonial form with non-motile cells embedded in a mucilage matrix several mm in diameter, to single, motile cells from 3 to 9 μm in size [Matrai et al., 1995]. Matrai et al. [1995] found that > 50% of carbon fixed by Phaeocystis can be allocated to

extracellular mucilage during the colonial life stage and that low molecular weight carbohydrates accumulate in the mucilage. Thus sinking Phaeocystis colonies can be efficient exporters of carbon from surface waters with C/N production ratios well above the typical Redfield ratio seen in most phytoplankton [Smith et al., 1996, 1999]. Phaeocystis spp. overwinter within the pack ice, and the ice age SIZ expansion would likely extend their range northward with the sea ice [Gibson et al., 1990]. This "seed stock" from melting sea ice and high photosynthetic efficiencies at low light levels often allows Phaeocystis to dominate early spring phytoplankton blooms in polar regions today [Gibson et al., 1990; Smith et al., 1991; 1999; Crocker et al., 1995; Smith and Gordon, 1997]. In the Antarctic, dense Phaeocystis blooms occur mainly in coastal/shelf waters, which may be related to iron availability [Smith et al., 1999]. Surface to volume ratio considerations suggest that the colonial form of Phaeocystis in particular may have difficulty obtaining necessary iron over much of the Southern Ocean [Sunda and Huntsman, 1997]. Thus the combination of elevated aeolian iron inputs and expansion of the SIZ during the last ice age probably led to a range expansion and increased production by Phaeocystis sp. [Martin, 1990; Gibson et al., 1990].

There is some evidence for this range expansion in the ice core record. Phaeocystis spp. are important producers of dimethylsulfoniopropionate (DMSP), which is a major source of cloud condensation nuclei, after conversion to dimethyl sulphide (DMS) [Charlson et al., 1987; Gibson et al., 1990]. During glacial stages, the atmospheric content of non-seasalt sulphate (NSS sulphate) recorded in ice cores from the Antarctic was ~20-46% higher than in the modern era, likely due to increased production of DMSP by marine biota [Legrand et al., 1988; 1991]. Phaeocystis forms an important component of the ice algae in the Southern Ocean, where it produces substantial amounts of DMSP, much of which is released to the water column during spring ice melt [Kirst et al., 1991]. Phaeocystis blooms result in high oceanic DMS concentrations and consequently high DMS fluxes to the atmosphere [Gibson et al., 1990; Crocker et al., 1995; Turner et al., 1995]. Thus an ice age range expansion and increase in primary production by Phaeocystis could account for the LGM increase in NSS sulphate in Antarctic ice core data reported by Legrand et al. [1988, 1991]. The primary oxidation products of DMS in the atmosphere are SO_2 (which is then converted to NSS sulphate) and methanesulphonate (MSA) [Legrand et al., 1991]. In the modern ocean, the molar ratio of MSA/NSS sulphate increases with latitude in the Southern Hemisphere, likely due to air temperature effects on DMS oxidation processes [Bates et al., 1992]. Thus the significantly higher MSA/NSS sulphate ratios in glacial Antarctic ice cores are also consistent with increased high latitude oceanic DMS production by Phaeocycstis [Legrand, 1997].

7.4. The Subantarctic Water Ring: From the PF to the North Subtropical Front

The primary factors affecting primary productivity in this region at the LGM were the increased deposition of atmospheric iron and the substantially cooler SST. The increased iron input to these waters would likely increase primary and export production [Martin, 1990; Sunda and Huntsman, 1997]. As discussed previously, cooler SST

values and possibly lower silica requirements may have enabled a northward range expansion by Antarctic diatoms.

There is substantial evidence that Subantarctic primary production was increased at the LGM. The sedimentary record for Subantarctic waters consistently shows increased biogenic opal and/or organic carbon flux to the sediments at the LGM [Mortlock et al., 1991; Charles et al., 1991; Kumar et al., 1993, 1995; Nelson et al., 1993; Rosenthal et al., 1995, 1997; Francois et al., 1997; Anderson et al., 1998]. Francois et al. [1992] argue for increased nutrient consumption in Subantarctic waters of the Indian sector during glacial times. Kumar et al. [1995] noted that the increased flux of organic carbon to the sediments at the LGM exceeded the increase in biogenic opal over much of the Subantarctic. Increased C/Si ratios in diatoms due to relief of iron stress may have played a role [Takeda, 1998]. Kumar et al. [1995] also estimated iron flux to the sediments in the Atlantic sector was ~5 times higher at the LGM. This elevated iron flux was attributed to increased aeolian deposition of iron from terrestrial sources on the South American continent [Kumar et al., 1995]. The flux of organic carbon to the sediments was also greatly increased in this region, by a factor of 4 over the area from 42°–54°S [Anderson et al., 1998].

8. Air-Sea CO$_2$ fluxes at the LGM

As noted in section 7.4, available evidence indicates that export production in Subantarctic waters was higher at the LGM and that this increase was stimulated by the increased atmospheric deposition of iron as postulated by Martin [1990] [Mortlock et al., 1991; Charles et al., 1991; Kumar et al., 1993, 1995; Nelson et al., 1993; Rosenthal et al., 1995, 1997; Francois et al., 1992, 1997; Anderson et al., 1998]. This would increase the flux of atmospheric CO$_2$ into Subantarctic waters particularly during spring/summer months, when production would be at a maximum.

Changes in ecosystem structure could also affect air-sea fluxes of CO$_2$ if they altered the mean CaCO$_3$/organic C ratio of sinking matter, which would alter surface alkalinity [Howard and Prell, 1994]. Lowering this ratio would result in increased alkalinity and reduced pCO$_2$ in surface waters [Howard and Prell, 1994]. Lower CaCO$_3$ accumulation rates [Nelson et al., 1993; Howard and Prell, 1994] and increased opal and organic carbon fluxes [Mortlock et al., 1991; Charles et al., 1991; Kumar et al., 1995; Anderson et al., 1998] to Subantarctic sediments imply that the ratio of CaCO$_3$/C$_{org}$ in sinking matter was lower at the LGM. This would have further enhanced the flux of CO$_2$ into the ocean [Howard and Prell, 1994]. This region therefore would have been a significantly stronger sink for atmospheric CO$_2$ at the LGM.

South of the PF, the situation becomes more complicated, and interactions between the sea ice and the biota over seasonal timescales would strongly affect net air-sea fluxes of CO$_2$. Air-sea fluxes of CO$_2$ through the pack ice are negligible compared with open water areas [Weiss, 1987; Augstein, 1994]. There was likely a strong flux of CO$_2$ into the oceans during austral spring and summer (due to relatively intense phytoplankton blooms driven by sea ice retreat and increased iron deposition) and a negligible net flux for much of the rest of the year because

of heavy sea ice cover. This is the pattern recently suggested for the southern Ross Sea [Bates et al., 1998]. Net CO$_2$ flux into the ocean would thus increase, even if annual export production remained at similar levels or even declined. A significant fraction of this production increase during austral spring/summer was likely due to Phaeocystis and would leave little in the way of sedimentary record [Martin, 1990].

In addition, physical factors associated with the expanded SIZ would have decreased the outgassing of CO$_2$ to the atmosphere at high southern latitudes during austral fall/winter. Persistent ice-cover would act as a physical barrier to air-sea gas exchange and may have reduced the upwelling rate of carbon rich waters at the AD by decreasing the momentum flux to surface waters during winter months. Increased vertical stratification during the spring ice melt could also reduce the mixing of carbon-rich waters into the surface layer [Francois et al., 1997].

A schematic summarizing these suggested ice age primary production patterns and their effect on air-sea fluxes of CO$_2$ is presented in Figure 1. By necessity Figure 1 represents a simplification; for example, within the SWR and PFR there are regions of elevated export production and strong CO$_2$ drawdown. However, mean chlorophyll concentrations indicate an overall pattern similar to that presented here (compare Plate 3 and Figure 1). The LGM pattern 'for the SWR (not shown) would be similar to the modern pattern but with a stronger seasonal cycle, peaking during summer. As noted previously, the POOZ did not exist at the LGM. The entire area from the PF south to the Antarctic continent was shifted toward the pattern seen in the Weddell-Ross Region today. There would be a strong flux of CO$_2$ into the oceans during the ice-free growing season and little net flux the rest of the year due to heavy ice cover (Figure 1). The length of the ice-free growing season would vary with latitude, with a progressively decreased ice-free season as one moved poleward. Thus the four ecological regions from the PF south to the Antarctic continent outlined by Tréguer and Jacques [1992] were replaced by one large SIZ at the LGM. The type of ecological regime shift suggested here, from a small phytoplankton dominated assemblage to one dominated by larger diatom species, has been documented for the glacial North Pacific [Sancetta, 1992]. Sancetta [1992] suggested relief from iron-limitation as a possible cause of the glacial shift toward larger diatoms and a higher productivity regime. The Subarctic North Pacific is also a HNLC region in the modern ocean [Martin, 1992].

Increasing primary and export production over the region south of the PF to values approaching what is observed in the Weddell-Ross Region today would result in a globally significant sink for atmospheric CO$_2$. Evidence for this is seen in the many modeling studies of such production increases in Southern Ocean waters [i.e., Sarmiento and Toggweiler, 1984; Sarmiento and Orr, 1991; Joos and Siegenthaler, 1991]. Some simple calculations can illustrate the potential impact of the proposed ecological regime shift on export production. Nelson et al. [1996] estimated a seasonally integrated f ratio of 0.42 and a total annual primary production of 142 g C m^{-2} yr^{-1} for the Ross Sea Shelf area. This indicates an annual export production of ~60 g C m^{-2} yr^{-1}. This production occurs over an ~6 month growing season and typically does not result in full depletion of macronutrients [Nelson et al., 1996]. If a
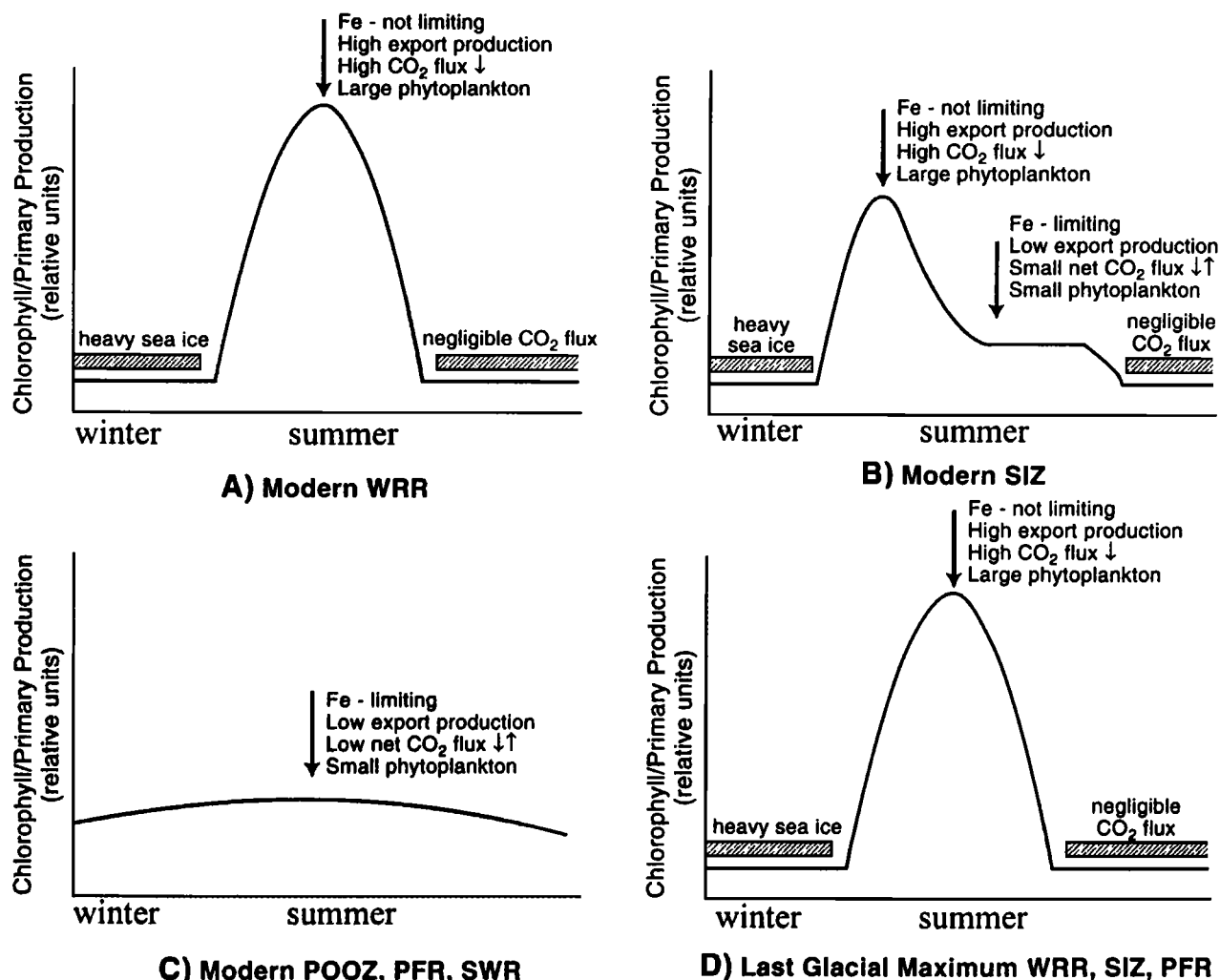
A) Modern WRR

Chlorophyll/Primary Production (relative units)

Fe - not limiting
High export production
High CO_2 flux ↓
Large phytoplankton

heavy sea ice

negligible CO_2 flux

winter   summer

B) Modern SIZ

Chlorophyll/Primary Production (relative units)

Fe - not limiting
High export production
High CO_2 flux ↓
Large phytoplankton

Fe - limiting
Low export production
Small net CO_2 flux ↓↑
Small phytoplankton

heavy sea ice

negligible CO_2 flux

winter   summer

C) Modern POOZ, PFR, SWR

Chlorophyll/Primary Production (relative units)

Fe - limiting
Low export production
Low net CO_2 flux ↓↑
Small phytoplankton

winter   summer

D) Last Glacial Maximum WRR, SIZ, PFR

Chlorophyll/Primary Production (relative units)

Fe - not limiting
High export production
High CO_2 flux ↓
Large phytoplankton

heavy sea ice

negligible CO_2 flux

winter   summer

Figure 1. Displayed is a schematic of proposed seasonal patterns in primary and export production, dominant phytoplankton size class, and air-sea carbon dioxide flux in different ecological regions of the Southern Ocean during the modern era and at the last glacial maximum. Air-sea flux through

similar export production occurred over the entire SIZ during the last ice age (30.7 million km^2, total area of the WRR, SIZ, POOZ, and PFR from Table 1), the annual carbon export from surface waters would have been 1.84 x 10^{15} gC yr^{-1}, or 1.84 Gt C yr^{-1}. Smith [1991] estimates new production for this region today as 0.47 Gt C yr^{-1}. Minas and Minas [1992] estimate nitrate-based new production for Antarctic waters as 30.2 g C m^{-2} yr^{-1} over the growing season from winter to late summer, which would correspond to 0.93 Gt C yr^{-1} over 30.7 million km^2. Wefer and Fischer [1991] estimated export flux at 100 m depth for the Southern Ocean from sediment trap data at 0.17 Gt C yr^{-1}. Thus carbon export south of the PF could have increased by ~0.9-1.6 Gt C yr^{-1} at the LGM. This level of increased export production would still not have fully utilized available macronutrients. Much of this exported carbon would be replaced by atmospheric CO_2 entering the ocean. Increased production by Phaeocystis sp. and higher C/Si ratios in diatoms at the LGM would both tend to minimize the sedimentary signal from this increased export production.

Increased export production north of the PF could also have global significance because of the large area covered by

Subantarctic waters (SWR is 48.7 million km^2 from Table 1). Current estimates for total primary production over most of this region today are in the range of 50-150 g C m^{-2} yr^{-1} [Antoine et al., 1996; Behrenfeld and Falkowski, 1997]. Banse [1996] noted that the f ratio in the SWR ranges between 0.3-0.5. Taking a mean annual production of 100 g C m^{-2} yr^{-1} and a mean f ratio of 0.4 gives an annual export production of ~40 g C m^{-2} yr^{-1}. Export production from the modern SWR would then amount to ~2.0 Gt C yr^{-1}. The data of Kumar et al. [1995] suggest a large increase in export production (by at least a factor of 2) at the LGM [see also Rosenthal et al., 1995]. Anderson et al. [1998] found a four-fold LGM increase in organic carbon accumulation in Subantarctic sediments. A doubling of export production would increase exported carbon from these waters to 4.0 Gt C yr^{-1}.

Thus, if export production doubled within the SWR and increased by ~0.9-1.6 Gt C yr^{-1} in waters farther south, export production from the entire Southern Ocean would have been some ~2.9-3.6 Gt C yr^{-1} greater at the LGM than at present. Martin [1990] estimated that the observed drawdown of atmospheric CO_2 during the last ice age

represented a ~170 Gt C flux out of the atmosphere. The estimated increase in Southern Ocean export production calculated above could have rapidly removed this amount of CO_2. These calculations represent conservative estimates of carbon flux as they do not require full utilization of macronutrients in Antarctic waters and do not include the effects of an expanded winter sea ice extent on outgassing of CO_2.

9. Conclusions

In summary, the Southern Ocean was a significantly stronger sink for atmospheric CO_2 during the last ice age and contributed substantially to the observed lowering of atmospheric CO_2 levels. Available evidence indicates that the increased atmospheric deposition of iron led to increased export production and consequently a stronger drawdown of atmospheric CO_2 in Subantarctic waters [Kumar et al., 1995; Anderson et al., 1998]. South of the PF, increased iron deposition and the effects of the greatly expanded seasonal ice sheet appear to have led to an intensification of phytoplankton blooms, increasing nitrate utilization from ~30 to ~70% as estimated by Francois et al. [1997]. This would result in a strong sink for atmospheric CO_2 due to biological production during the shortened growing season of the LGM, as happens today in the southern Weddell and Ross Seas [Takahashi et al., 1993, 1997; Bates et al., 1998]. With minimal air-sea fluxes of CO_2 the rest of the year because of persistent sea ice cover, the entire region south of the PF would have been a significantly stronger sink for atmospheric CO_2 than in the modern ocean. We have argued that the total biological export of carbon from surface waters south of the PF was higher at the LGM than at present. However, even areas where annual export production declined could be stronger net sinks for atmospheric CO_2 than at present due to the interactions between the sea ice and biota over seasonal timescales.

Additional analysis of sediment cores will improve our understanding of Southern Ocean ecology at the LGM. New paleoproductivity studies in the Pacific sector and south of ~60°S should be a high priority, as there is relatively little data available at present. Further examination of the geological record will also improve estimates of summer sea ice extent at the LGM and could be used to test our hypothesis that maximum winter ice extent was at or only slightly north of the modern mean PF location.

The aeolian flux of iron to the oceans is much lower in the Pacific sector than in the Atlantic and Indian basins [Duce and Tindale, 1991]. Thus it is in the Pacific basin that the strongest biological response to the elevated LGM dust fluxes should have occurred. New paleoceanographic techniques hold promise for testing the hypothesis that phytoplankton growth rates were increased in glacial times due to this increased iron flux from the atmosphere [Bidigare et al., 1999].

Sedimentary records integrate over long time periods, however, and provide limited information about the seasonal interactions between sea ice and the biota discussed here. Ultimately, our best hope for defining the role of the Southern Ocean in the glacial lowering of atmospheric CO_2 may lie in the realm of modeling. A general circulation model of the LGM climate that incorporates realistic biota and sea ice dynamics could provide valuable insights and greatly enhance our interpretation of the geological record.

References

Anderson, RF, N. Kumar, R.A. Mortlock, P.N. Froelich, P. Kubik, B. Dittrich-Hannen, and M. Suter, Late-Quaternary changes in productivity of the Southern Ocean, J. Mar. Syst., 17, 497-514, 1998.

Antoine, D., A. Jean-Michel, and A. Morel, Oceanic primary production 2. Estimation at global scale from satellite (coastal zone color scanner) chlorophyll, Global Biogeochem. Cycles, 10, 57-69, 1996.

Arrigo, KR, D. Worthen, A. Schnell, and M.P. Lizotte, Primary production in Southern Ocean waters, J. Geophys. Res., 103, 15587-15600, 1998.

Augstein, E, Future Ocean-atmosphere research in the Antarctic region, in Antarctic Science – Global Concerns, edited by G. Hempel, pp. 278-282, Springer-Verlag, New York, 1994.

Bakker, D.C.E., H.J.W. De Baar, and U.V. Bathmann, Changes of carbon dioxide in surface waters during spring in the Southern Ocean, Deep Sea Res. Part II, 44, 91-127, 1997.

Banse, K, Low seasonality of low concentrations of surface chlorophyll in the Subantarctic water ring: Underwater irradiance, iron, or grazing?, Prog. Oceanogr., 37, 241-291, 1996.

Bard, E., B. Hamelin, R.G. Fairbanks, and A. Zindler, Calibration of ^{14}C timescale over the past 30,000 years using mass spectrometric U-Th ages from Barbados corals, Nature 345, 405-410, 1990.

Barnola, J.M., D. Raynaud, Y.S. Korotkevich, and C. Lorius, Vostok ice core provides 160,000-year record of atmospheric CO_2, Nature, 329, 408-413, 1987.

Bates, N.R., D.A. Hansell, C.A. Carlson, and L.I. Gordon, Distribution of CO_2 species, estimates of net community production, and air-sea CO_2 exchange in the Ross Sea polynya, J. Geophys. Res., 103 2883-2896, 1998.

Bates, T.S., J.A. Calhoun, P.K. Quinn, Variations in the methansulfonate to sulfate molar ratio in submicrometer marine aerosal particles over the South Pacific Ocean, J. Geophys. Res., 97, 9859-9865, 1992.

Behrenfeld, M.J., and P.G. Falkowski, Photosynthetic rates derived from satellite-based chlorophyll concentration, Limnol. Oceanogr., 42, 1-20, 1997.

Belkin, I.M., and A.L. Gordon, Southern Ocean fronts from the Greenwich meridian to Tasmania, J. Geophys. Res., 101, 3675-3696, 1996.

Bidigare, R.R., et al., Iron-stimulated changes in ^{13}C fractionation and export by equatorial Pacific phytoplankton: Toward a paleo-growth rate proxy, Paleoceanogr., (in press), 1999.

Bouquegneau, J.M., W.W.C. Gieskes, G.W. Kraay, and A.M. Larsson, Influence of physical and biological processes on the concentration of O_2 and CO_2 in the ice-covered Weddell Sea in the spring of 1988, Polar Biol., 12, 163-170, 1992.

Boyd, P., A. Watson, and C. Law, Spotlight is on iron at international SOIREE in Southern Ocean, U.S. JGOFS Newsletter, 9, 10-11, 1999.

Howard, W.R., and W.L. Prell, Late quaternary surface circulation of the Southern Indian Ocean and its relationship to orbital variations, *Paleoceanography, 7,* 79-117, 1992.

Howard, W.R., and W.L. Prell, Late Quaternary CaCO₃ production and preservation in the Southern Ocean: Implications for oceanic and atmospheric carbon cycling, *Paleoceanography, 9,* 453-482, 1994.

Hutchins, D.A., and K.W. Bruland, Iron-limited growth and Si:N uptake ratios in a coastal upwelling regime, *Nature, 393,* 561-564, 1998.

Hutchins, D.A., G.R. DiTullio, Y. Zhang, and K.W. Bruland, An iron limitation mosaic in the California upwelling regime, *Limnol. Oceanogr., 43,* 1037-1054, 1998.

Ikehara, M., K. Kawamura, N. Ohkouchi, K. Kimoto, M. Murayama, T. Nakamura, T. Oba, T, and A. Taira, Alkenone sea surface temperature in the Southern Ocean for the last two deglaciations, *Geophys. Res. Lett., 24,* 679-682, 1997.

Inoue, H.Y., and Y. Sugimura, Distribution and variations of oceanic carbon dioxide in the western North Pacific, eastern Indian, and Southern Ocean south of Australia, *Tellus Ser. B, 40B,* 308-320, 1988.

Ishii, M., H.Y. Inoue, H. Matsueda, and E. Tanoue, Close coupling between seasonal biological production and dynamics of dissolved inorganic carbon in the Indian Ocean sector and the western Pacific sector of the Antarctic Ocean, *Deep Sea Res. Part I., 45,* 1187-1209, 1998.

Jennings Jr, J.C., L.I. Gordon, and D.M. Nelson, Nutrient depletion indicates high primary productivity in the Weddell Sea, *Nature, 308,* 51-54, 1984.

Joos, F., and U. Siegenthaler, Possible effects of iron fertilization in the Southern Ocean on atmospheric CO₂ concentration, *Global Biogeochem. Cycles, 5,* 135-150, 1991.

Jordon, R.W., and C.J. Pudsey, High-resolution diatom stratigraphy of Quaternary sediments from the Scotia Sea, *Mar. Micropaleontol., 19,* 201-237, 1992.

Jouzel, J., C. Lorius, J.R. Petit, C. Genthon, N.I. Barkov, V.M. Kotlyakov, and V.M. Petrov, Vostok ice core: a continuous isotope temperature record over the last climatic cycle (160,000 years), *Nature 329,* 403-407, 1987.

Keir, R.S., On the late Pleistocene oocean geochemistry and circulation, *Paleoceanography, 3,* 413-445, 1988.

Kellogg, T.B., Glacial-interglacial changes in global deepwater circulation, *Paleoceanography, 2,* 259-271, 1987.

Kirst, G.O., C. Thiel, H. Wolff, J. Nothnagel, M. Wanzek, and R. Ulmke, Dimethylsulfoniopropionate (DMSP) in ice-algae and its possible biological role, *Mar. Chem., 35,* 381-388, 1991.

Klinck, J.M., and D.A. Smith, DA, Effect of wind changes during the last glacial maximum on the circulation in the Southern Ocean, *Paleoceanography, 8,* 427-433, 1993.

Knox, F., and M.B. McElroy, Changes in atmospheric CO₂: Influence of the marine biota at high latitude, *J. Geophys. Res., 89,* 4629-4637, 1984.

Kumar, N., R. Gwiazda, R.F. Anderson, and P.N. Froelich, ²³¹Pa/²³⁰Th ratios in sediments as a proxy for past changes in Southern Ocean productivity. *Nature, 362,* 45-48, 1993.

Kumar, N., R.F. Anderson, R.A. Mortlock, P.N. Froelich, P. Kubik, B. Dittrich-Hannen, and M. Suter, Increased biological productivity and export production in the glacial Southern Ocean. *Nature, 378,* 675-680, 1995.

Labeyrie, L, et al., Hydrographic changes of the Southern Ocean (southeast Indian sector) over the last 230 kyr, *Paleoceanography, 11,* 57-76, 1996.

Landry, M.R., et al., Iron and grazing constraints on primary production in the central equatorial Pacific: An EqPac synthesis, *Limnol. Oceanogr., 42,* 405-418, 1997.

Laubscher, R.K., R. Perisinotto, and C.D. McQuaid, Phytoplankton production and biomass at frontal zones in the Atlantic sector of the Southern Ocean, *Polar Biol., 13,* 471-481, 1993.

Legrand, M.R., Ice-core records of atmospheric sulphur, *Phil. Trans. Roy. Soc. Lon. B, 352,* 241-250, 1997.

Legrand, M.R., R.J. Delmas, and R.J. Charlson, Climate forcing implications from Vostok ice-core sulphate data, *Nature, 334,* 418-420, 1988.

Legrand, M., C. Feniet-Saigne, E.S. Saltzman, C. Germain, N.I. Barkov, V.N. Petrov, Ice-core record of oceanic emissions of dimethylsulphide during the last climate cycle, *Nature, 350,* 144-146, 1991.

Löscher, B.M., H.J.W. de Baar, J.T.M. de Jong, C. Veth, and F. Dehairs, The distribution of Fe in the Antarctic Circumpolar Current, *Deep Sea Res Part II, 44,* 143-187, 1997.

Lutjeharms, J.R.E., N.M. Walters, and B.R. Allanson, Oceanic frontal systems and biological enhancement, In: *Antarctic Nutrient Cycles and Food Webs,* edited by W.R. Siegfried, P.R. Condy, and R.M. Laws, pp. 11-21, Springer-Verlag, Berlin, 1985.

Mackensen, A., H. Grobe, H.W. Hubberten, and G. Kuhn, Benthic foraminiferal assemblages and the δ³ C-signal in the Atlantic Sector of the Southern Ocean: Glacial-to-interglacial contrasts, In: Carbon Cycling in the Glacial Ocean: Constraints on the Ocean's Role in Global Change, edited by R. Zahn et al., Springer-Verlag, Berlin Heidelberg, p. 105-135, 1994.

Martin, J.H., Glacial-interglacial CO₂ change: The Iron hypothesis. *Paleoceanography, 5,* 1-13, 1990.

Martin, J.H., Iron as a limiting factor in oceanic productivity, In: *Primary Productivity and Biogeochemical Cycles in the Sea,* edited by P.G. Falkowski, and A.D. Woodhead, pp. 123-137, Plenum Press, New York, 1992.

Martin, J.H., S.E. Fitzwater, and R.M. Gordon, Iron in Antarctic waters. *Nature, 345,* 156-158, 1990a.

Martin, J.H., S.E. Fitzwater, and R.M. Gordon, Iron deficiency limits phytoplankton growth in Antarctic waters, *Global Biogeochem. Cycles, 4,* 5-12, 1990b.

Martinson, D.G., Evolution of the Southern Ocean winter mixed layer and sea ice: Open ocean deepwater formation and ventilation, *J. Geophys. Res., 95,* 11641-11654, 1990.

Matrai, P.A., M. Vernet, R. Hood, A. Jennings, E. Brody, S. Saemundsdóttir, Light-dependence of carbon and sulfur production by polar clones of the genus *Phaeocystis, Mar. Biol., 124,* 157-167, 1995.

McClain, C..R, M.L. Cleave, G.C. Feldman, W.W. Gregg, S.B. Hooker, and N. Kuring, Science quality SeaWiFS data for global biosphere research, *Sea Tech.,* September, 10-16, 1998.

Metzl, N., C. Beauverger, C. Brunet, C. Goyet, and A. Poisson, Surface water carbon dioxide in the southwest Indian sector of the Southern Ocean: a highly variable CO₂ source/sink region in summer, *Mar. Chem., 35,* 85-95, 1991.

Metzl, N., A. Poisson, F. Louanchi, C. Brunet, B. Schauer, and B. Bres, Spatio-temporal distributions of air-sea fluxes of CO₂ in the Indian and Antarctic Oceans, *Tellus Ser. B, 47B,* 56-69, 1995.

Minas, H.J., and M. Minas Net community production in "High Nutrient-Low Chlorophyll" waters of the tropical and Antarctic Oceans: grazing vs. iron hypothesis, *Oceanol. Acta, 15,* 145-162, 1992.

Moore, J.K., M.R. Abbott, J.G. Richman, Variability in the location of the Antarctic Polar Front (90°-20°W) from satellite sea surface temperature data, *J. Geophys. Res. 102,* 27825-27833, 1997.

Moore, J.K., M.R. Abbott, and J.G. Richman, Location and dynamics of the Antarctic Polar Front from satellite sea surface temperature data, *J. Geophys. Res., 104,* 3059-3073, 1999a.

Moore, J.K., M.R. Abbott, J.G. Richman, W.O. Smith, T.J. Cowles, K.H. Coale, W.D. Gardner, and R.T. Barber, SeaWiFS satellite ocean color data from the Southern Ocean, *Geophys. Res. Lett., 26,* 1465-1468, 1999b.

Morley, J.J., Variations in high-latitude oceanographic fronts in the Southern Indian Ocean: An estimation based on faunal changes, *Paleoceanography, 4,* 547-554, 1989.

Mortlock, R.A., C.D. Charles, P.N. Froelich, M.A. Zibello, J. Saltzman, J.D. Hays, and L.H. Burckle, Evidence for lower productivity in the Antarctic Ocean during the last glaciation, *Nature, 351,* 220-223, 1991.

Murphy, P.P., R.A. Feely, R.H. Gammon, K.C. Kelly, and L.S. Waterman, Autumn air-sea disequilibrium of CO₂ in the South Pacific Ocean, *Mar. Chem., 35,* 77-84, 1991.

National Snow and Ice Data Center, Passive Microwave Derived Monthly Polar Sea Ice Concentration Time Series, Digital data

available from nsidc@kryos.colorado.edu, Boulder, Colorado, NSIDC Distributed Active Archive Center, Univ. of Colo. at Boulder, 1998.

Nelson, C.S., P.J. Cooke C.H. Hendy, and A.M. Cuthbertson, AM, Oceanographic and climatic changes over the past 160,000 years at deep sea drilling project site 594 off southeastern New Zealand, southwest Pacific Ocean, *Paleoceanography*, 8, 435-458, 1993.

Nelson, D.M., D.J. DeMaster, R.B. Dunbar, and W.O. Smith Jr, Cycling of organic carbon and biogenic silica in the Southern Ocean: Estimates of water-column and sedimentary fluxes on the Ross Sea continental shelf, *J. Geophys. Res.*, *101*, 18519-18532, 1996.

Nelson, D.M., and W.O. Smith Jr., Phytoplankton bloom dynamics of the western Ross Sea ice edge - II. Mesoscale cycling of nitrogen and silicon, *Deep Sea Res. Part I.*, 33, 1389-1412, 1986.

Neori, A., and O. Holm-Hansen, Effect of temperature on rate of photosynthesis in Antarctic phytoplankton, *Polar Biol.*, 1, 33-38, 1982.

Nicol, S., I. Allison, The Frozen skin of the Southern Ocean, *Am. Sci.*, 85, 426-439, 1997.

Nolting, R.F., H.J.W. de Baar, A.J. Van Bennekom, and A. Masson, Cadmium, copper and iron in the Scotia Sea, Weddell Sea, and Weddell/Scotia Confluence (Antarctica), *Mar. Chem.*, 35, 219-243, 1991.

Nürnberg, C..C, G. Bohrmann, M. Schlüter, and M. Frank, Barium accumulation in the Atlantic sector of the Southern Ocean: Results from 190,000-year records, *Paleoceanography*, 12, 594-603, 1997.

Petit, J.R., M. Briat, and A. Royer, Ice age aerosol content from East Antarctic ice core samples and past wind strength, *Nature*, 293, 391-394, 1981.

Petit, J.R., L. Mounier, J. Jouzel, Y.S. Korotkevich, V.I. Kotlyakov, and C. Lorius, Palaeoclimatological and chronological implications of the Vostok core dust record, *Nature*, 343, 56-58, 1990.

Pichon, J.J., M. Labeyrie, G. Bareille, M. Labracherie, J. Duprat, and J. Jouzel, Surface water temperature changes in the high latitudes of the southern hemisphere over the last glacial-interglacial cycle, *Paleoceanography*, 7, 289-318, 1992.

Poisson A., N. Metzl, X. Danet, F. Louanchi, C. Brunet, B. Schauer, B. Brés, and D. Ruiz-Pino, Air-sea CO₂ fluxes in the Southern Ocean Between 25°E and 85°E, in *The Polar Oceans and Their Role in Shaping the Global Environment, Geophys. Monogr. 85*, edited by O.M. Johannessen et al., pp. 273-284, AGU Washington D.C., 1994.

Prell, W.L., W.H. Hutson, D.F. Williams, A.W.H. Bé, K. Geitzenauer, and B. Molfino, Surface circulation of the Indian Ocean during the last glacial maximum, Approximately 18,000 yr B.P., *Quat. Res.*, 14, 309-336, 1980.

Redfield, A.C., B.H. Ketchum, and F.A. Richards, The Influence of organisms on the composition of seawater, in *The Sea*, Vol. 2, edited by M.N. Hill, pp. 26-77, Wiley Interscience, New York, 1963.

Robertson, J.E., and A.J. Watson, A summer-time sink for atmospheric carbon dioxide in the Southern Ocean between 88 °W and 80 °E, *Deep Sea Res. Part II*, 42, 1081-1091, 1995.

Rosenthal, Y., E.A. Boyle, L. Labeyrie, and D. Oppo, Glacial enrichments of authigenic Cd and U in Subantarctic sediments: A climatic control on the elements' oceanic budget?, *Paleoceanography*, 10, 395-413, 1995.

Rosenthal, Y., E.A. Boyle, and L. Labeyrie, Last glacial maximum paleochemistry and deepwater circulation in the Southern Ocean: Evidence from foraminiferal cadmium, *Paleoceanography*, 12, 787-796, 1997.

Rubin, S., J. Goddard, D. Chipman, and T. Takahashi, Carbon dioxide partial pressure in surface waters in the Pacific sector of the southern oceans during austral summers 1992 and 1994, *Antarct. J. U.S.*, 31, 113-115, 1994.

Sabine, C.L., and R.M. Key, Controls on f_{CO_2} in the South Pacific, *Mar. Chem.*, 60, 95-110, 1998.

Sancetta, C., Primary production in the glacial North Atlantic and North Pacific oceans, *Nature*, 360, 249-251, 1992.

Sarmiento, J.L., and J.R. Toggweiler, A new model for the role of the oceans in determining atmospheric P_{CO_2}, *Nature*, 308, 621-624, 1984.

Sarmiento, J.L., and J.C. Orr, Three-dimensional simulations of the impact of Southern Ocean nutrient depletion on atmospheric CO₂ and ocean chemistry, *Limnol. Oceanogr.*, 36, 1928-1950, 1991.

Sarmiento, J.L., and C. Le Quéré, Oceanic carbon dioxide uptake in a model of century-scale global warming, *Science*, 274, 1346-1350, 1996.

Scharek, R., M.A. Van Leeuwe, and H.J.W. De Baar, Responses of Southern Ocean phytoplankton to the addition of trace metals, *Deep-Sea Res. Part II*, 44, 209-228, 1997.

Sedwick, P.N., P.R. Edwards, D.J. Mackey, F.B. Griffiths, and J.S. Parslow, Iron and manganese in surface waters of the Australian subantarctic region, *Deep-Sea Res. I.*, 44, 1239-1253, 1997.

Sedwick, P.N., and G.R. DiTullio, Regulation of algal blooms in Antarctic Shelf waters by the release of iron from melting sea ice, *Geophys. Res. Lett.*, 24, 2515-2518, 1997.

Sedwick, P..N, G.R. DiTullio, and D. Mackey, Dissolved iron and manganese in surface waters of the Ross Sea, austral summer 1995-1996, *Ant. J. of the U.S.*, 31, 128-130, 1996.

Shemesh, A., S.A. Macko, C.D. Charles, and G.H. Rau, Isotopic evidence for reduced productivity in the Glacial Southern Ocean, *Science*, 262, 407-410, 1993.

Sherr, E.B., and B.F. Sherr, 1994, Bacterivory and herbivory: Key roles of phagotropic protists in pelagic food webs, *Microb. Ecol.*, 28, 223-235, 1994.

Shimmield, G., S. Derrick, A. Mackensen, H. Grobe, and C. Pudsey, The history of barium, biogenic silica and organic carbon accumulation in the Weddell Sea and Antarctic Ocean over the last 150,000 years, in *Carbon Cycling in the Glacial Ocean: Constraints on the Ocean's Role in Global Change*, edited by R. Zahn et al., pp. 555-574, Springer-Verlag, New York, 1994.

Siegenthaler, U., and T. Wenk, Rapid atmospheric CO₂ variations and ocean circulation, *Nature*, 308, 624-626, 1984.

Smetacek, V., R. Scharek, L.I. Gordon, H. Eicken, E. Fahrbach, G. Rohardt, and S. Moore, Early spring phytoplankton blooms in ice platelet layers of the southern Weddell Sea, Antarctica, *Deep Sea Res. Part I*, 39, 153-168, 1992.

Smith, S.D., R.D. Muench, and C.H. Pease, Polynyas and leads: An overview of physical processes and environment, *J. Geophys. Res.*, 95, 9461-9479, 1990.

Smith Jr, W.O., Nutrient distributions and new production in polar regions: Parallels and contrasts between the Arctic and Antarctic, *Mar. Chem.*, 35, 245-257, 1991.

Smith Jr., W.O, and L.I. Gordon, Hyperproductivity of the Ross Sea (Antarctica) Polynya during austral spring, *Geophys. Res. Lett.*, 24, 233-236, 1997.

Smith Jr., W.O., and D.M. Nelson, Phytoplankton bloom produced by a receding ice edge in the Ross Sea: Spatial coherence with the density field, *Science*, 227, 163-166, 1985.

Smith Jr., W.O., and D.M. Nelson, Importance of ice edge phytoplankton production in the Southern Ocean, *BioScience*, 36, 251-257, 1986.

Smith Jr., W.O., and D.M. Nelson, Phytoplankton growth and new production in the Weddell Sea marginal ice zone in the austral spring and autumn, *Limnol. Oceanogr.*, 35, 809-821, 1990.

Smith Jr., W.O., L.A. Codispoti, D.M. Nelson, T. Manley, E.J. Buskey, H.J. Niebauer, and G.F. Cota, Importance of *Phaeocystis* blooms in the high-latitude ocean carbon cycle, *Nature*, 352, 514-516, 1991.

Smith Jr., W.O., and E. Sakshaug, Polar phytoplankton, in *Polar Oceanography, Part B: Chemistry, Biology, and Geology*, edited by W.O. Smith, Academic Press, San Diego, Calif., 1990

Smith Jr., W.O., D.M. Nelson, G.R. DiTullio, and A.R. Leventer, Temporal and spatial patterns in the Ross Sea: Phytoplankton biomass, elemental composition, productivity and growth rates, *J. Geophys. Res.*, 101, 18455-18465, 1996.

Smith Jr., W.O., D.M. Nelson, and S. Mathot, Phytoplankton growth rates in the Ross Sea, Antarctica determined by independent methods: temporal variations, in press, *J. Plank. Res.*, 1999.

Sullivan, C.W., K.R. Arrigo, C.R. McClain, J.C. Comiso, and J. Firestone. Distributions of phytoplankton blooms in the Southern Ocean. *Science*, *262*, 1832-1837, 1993.

Sunda, W.G., and S.A. Huntsman, Interrelated influence of iron, light, and cell size on marine phytoplankton growth, *Nature*, *390*, 389-392, 1997.

Takahashi, T., J. Olafsson, J.G. Goddard, D.W. Chipman, and S.C. Sutherland, Seasonal variation of CO_2 and nutrients in the high-latitude surface oceans: A comparative study, *Global Biogeochem. Cyc.*, *7*, 843-878, 1993.

Takahashi, T., R.A. Feely, R.F. Weiss, RH. Wanninkhof, D.W. Chipman, S.C. Sutherland, and T.T. Takahashi, Global air-sea flux of CO_2: An estimate based on measurements of sea-air pCO_2 difference, *Proc. Natl. Acad. Sci.*, *94*, 8292-8299, 1997.

Takeda, S., Influence of iron availability on nutrient consumption ratio of diatoms in oceanic waters, *Nature*, *393*, 774-777, 1998.

Tréguer, P., and G. Jacques, Dynamics of nutrients and phytoplankton, and fluxes of carbon, nitrogen, and silicon in the Antarctic Ocean, *Polar Biol.*, *12*, 149-162, 1992.

Turner, S.M., P.D. Nightingale, W. Broadgate, and P.S. Liss, The distribution of dimethyl sulphide and dimethylsulphoniopropionate in Antarctic waters and sea ice, *Deep Sea Res. Part II*, *42*, 1059-1080, 1995.

Van Leeuwe, M..A, R. Scharek, H.J.W. De Baar, J.T.M. De Jong, and L. Goeyens, L, Iron enrichment experiments in the Southern Ocean: physiological responses of plankton communities, *Deep-Sea Res. II*, *44*, 189-208, 1997.

Wamser, C., and D.G. Martinson, Drag coefficients for winter Antarctic pack ice, *J. Geophys. Res.*, *98*, 12431-12437, 1993.

Watkins, N.D., M.T. Ledbetter, and T.C. Huang, Antarctic glacial history using spatial and temporal variations of ice-rafted debris in abyssal sediments of the Southern Ocean, in *Antarctic Geoscience*, edited by C. Craddock, pp. 1013-1016, Univ. of Wisc. Press, Madison, Wisc., 1982.

Weaver, P.P.E., L. Carter, and H.L. Neil, Response of surface water masses and circulation to late Quaternary climate change east of New Zealand, *Paleoceanography*, *13*, 70-83, 1998.

Wefer, G., and G. Fischer, Annual primary production and export flux in the Southern Ocean from sediment trap data, *Mar. Chem.*, *35*, 597-613, 1991.

Weiss, R.F., Winter Weddell Sea Project 1986: Trace gas studies during legs ANT V/2 and V/3 of *Polarstern*, *Antarct. J. of the U.S.*, *22*, 99-100, 1987.

Westerlund, S., and P. Öhman, Iron in the water column of the Weddell Sea, *Mar. Chem.*, *35*, 199-217, 1991.

Wilson, D.L., W.O. Smith Jr., and D.M. Nelson, Phytoplankton bloom dynamics of the western Ross Sea ice edge I. Primary productivity and species-specific production, *Deep Sea Res.*, *33*, 1375-1387, 1986.

Mark R. Abbott, James G. Richman, and David M. Nelson, College of Oceanic and Atmospheric Sciences, Oregon State University,104 Ocean Admin Building, Corvallis, OR, 97331-5503

J. K. Moore, National Center for Atmospheric Research, Advanced Studies Program, P.O. Box 3000, Boulder, CO, 80307. (jkmoore@cgd.ucar.edu)